POLITECNICO DI TORINO

Master's degree in Civil Engineering

A.y. 2021/2022

Experimental evaluation on the influence of cement-treated base materials components on physical and mechanical properties

Supervisor:

Prof. Ezio Santagata

Co-supervisors:

Prof. Davide Dalmazzo

Prof.ssa Lucia Tsantilis

Prof. Pier Paolo Riviera

Candidate:

Vanessa De Martini

Ai miei genitori,

per essere sempre stati al mio fianco ed avermi sostenuta.

Vi amo con tutto il cuore.

ABSTRACT

The rapid traffic growth, the consumption of natural resources, and environmental concerns are directing the design of future infrastructures to be economical and sustainable. In this regard, cement-treated base material increases pavements' bearing capacity and improves the load distribution to the underlying foundation. Its combination with an asphalt layer has excellent potential to guarantee a long life with minimum maintenance. Although several studies have been conducted to investigate the properties of cement-treated base material, the influence of its components is not totally clear to fully exploit this material's potential.

The primary purpose of this study is to evaluate the variation of mechanical and physical properties of cement-treated base materials at the variation of some parameters, such as the cement content, the water content, the lithic structure, and the compaction methodology. To achieve these objectives, a campaign of experimental tests is carried out in the Road Material Laboratory of the Polytechnic of Turin.

Four granular mixtures were designed. The first two were made by combining three aggregate classes (0/8, 8/18, and 18/30 mm) and were characterized by a very low fine content, while the other two were optimized by adding mineral filler. By selecting two of them, two cement-bound mixtures were designed to evaluate the influence of the cement dosage, which was varied in the range from 1,5% to 3,5%. A Proctor study on each considered mixture was conducted to investigate the influence of lithic skeleton and cement dosage on the optimum water content and dry density. Unconfined compressive and indirect tensile tests were performed on the cement-bounded mixtures to evaluate the effects of cement dosage on mechanical strength. Finally, additional ITS tests were made on selected mixtures on specimens compacted through the Gyratory compactor to investigate how the compaction methodology influences the results.

At the end of the experimental campaign, the linear relationship between the cement content and the physical and mechanical properties of the material, such as dry density, compressive strength, tensile strength, has been demonstrated. Moreover, the correlation with elastic parameters has been investigated, leading to the same results. Instead, the water content has the opposite effect on mechanical properties; indeed, its increase results

in linear degrowth of ITS. Furthermore, the lithic structure findings reveal a positive effect on the addition of filler on dry densities.

Finally, the additional tests on samples compacted through the Gyratory compaction apparatus have yielded interesting results; indeed, this compaction method improves the material's mechanical properties and achieves higher densities.

1 INDEX

INDEX OF FIGURES

INDEX OF TABLES

INDEX OF EQUATIONS

INTRODUCTION

The rapid traffic growth, the consumption of natural resources, and environmental concerns are directing the design of future infrastructures to be more economical, sustainable, and "maintenance-free." [2-4]

The terms "economic" and "sustainable" estimate the whole-life value of the pavement, even if measures of sustainable value are complex to assess because giving a monetary value to sustainability is not simple to date. Instead, the "maintenance-free" concept considers the functional state of the pavement, such as skid resistance and ride quality, and in structural terms, the reduction of pavement structural deterioration over time or caused by traffic. [4]

Indeed, nowadays, a fundamental goal in the pavement industry is to provide construction at ever lower life-cycle costs. The ambition of economic and sustainable infrastructures is to guarantee a longer service life, reducing distresses and leading to sporadic rehabilitation. However, this concept requires continuous advancement in design, material characterization, maintenance techniques, and management. [3]

Concurrently with this, one can talk about semi-rigid pavement constructions. These pavements gained popularity in Europe in the '70s when an escalation in the oil price led the unit cost of asphalt to grow. These pavements required less asphalt than the fully-flexible ones, so the celebrity was a merit of their economic efficiency. In the coming years, semi-rigid pavement's popularity comes for environmental reasons since hydraulically bound materials can use a broader range of aggregates and, therefore, be employed to maximize the consumption of locally available aggregates. Besides economic and environmental reasons, from a structural point of view, the rigid form of the base layer removes bottom-up fatigue cracking, rutting in the unbound layers, frost heave, and limits potential distresses such as cracking and rutting to the pavement surface, enhancing pavement durability. [3-5]

This research focuses on one of the most employed among the hydraulically bound materials, the "cement-treated base material," also known as C.T.B., widely used as the base layer for concrete or asphalt pavements. It consists of granular materials mechanically bonded by cement. Compared to unstabilized granular bases, it is stronger and more rigid, and therefore, it requires lower thicknesses even carrying the same traffic. Due to the strong uniform support that ensures, stresses applied to the subgrade are reduced. Moreover, loads distributed over a wider area lead to lower strains in the asphalt layer, reduced deflections, and delayed surface distresses onset. [3] [7] [10] [11].

The first chapter is entirely dedicated to a theoretical framework of the material. The objective is to comprehensively describe the cement-treated base materials, their primary uses, and peculiarities, highlighting the related advantages and disadvantages.

Instead, the second and the third chapters are devoted to the experimental campaign carried out in the Road Material Laboratory of the Polytechnic of Turin. The second focuses on the experimental plan's objectives and methodologies, while the third deals with experimental results.

Finally, the fourth chapter is dedicated to data analysis, and the last one is devoted to discussions and conclusions.

1 THEORETICAL FRAMEWORK

A cement-treated base (C.T.B.) is a strong, frost-resistant base layer for a concrete or asphalt pavement. It can be composed of existing or borrowed stone, gravel, sand, and silt, recycled concrete aggregates, recycled asphalt pavement, or manufactured aggregates with small amounts of cement and water that hardens after compaction and curing to form a durable, strong, frost resistant paving material. [7][9]

It is commonly known as cement-treated base, but other designations are sometimes used: soil-cement base, cement-treated aggregate base, cement-stabilized roadbed, and cement-stabilized base [10-12][19].

This material is relatively strong, durable, guarantees a good loads distribution to the underlying foundation, and represents a strong base for projects with specific durability and strength requirements. Therefore, it is extensively used as a pavement base for highways, roads, streets, parking areas, airports, industrial facilities, materials handling, and storage areas [7] [8] [10] [19].

It is mixed in-place and compacted after blending or mixed in a central plant or pugmill and then brought to the placement area, spread on a prepared subgrade or subbase, and compacted depending on the project requirement. The pavement structure is then completed by placing a bituminous or Portland cement concrete wearing course on top of the cured C.T.B. (Figure 1) [7] [11][19].

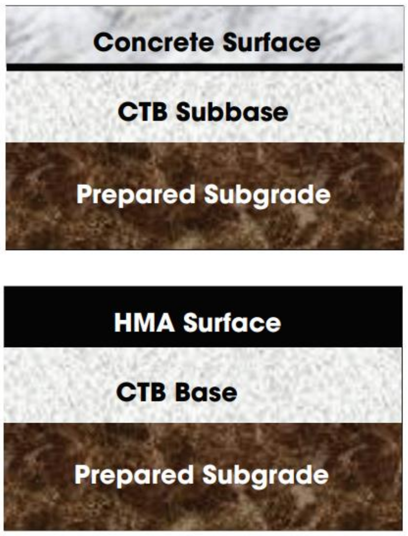

Figure 1- Typical pavement cross-sections [12]

In particular, the use of cement-treated base materials increases the bearing capacity of pavements, and the combination of a bound structural layer and an asphalt layer has excellent potential to provide long-life pavements with minimum maintenance [8].

Compared to an unstabilized granular base, C.T.B. is much stronger and more rigid [10] therefore requires lower thicknesses even carrying the same traffic. It can distribute loads over a wider area, reduce stresses on the subgrade and act as the load-carrying element of flexible pavement or a subbase for concrete (Figure 2) [7] [11].

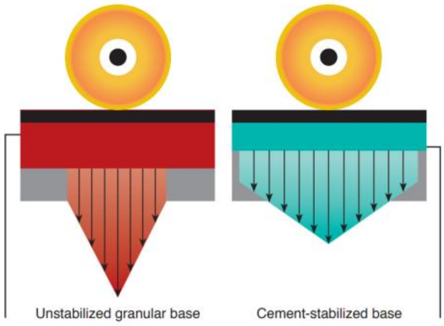

Figure 2- C.T.B. distribution of loads over a wider area [11]

A stiffer base reduces deflections caused by traffic loads, leading to lower strains in the asphalt surface, delaying the onset of surface distresses, and extending pavement life. Moreover, C.T.B. provides strong uniform support to reduce stresses applied to the subgrade. Despite an unstabilized granular base where rutting can occur in the surface, base, and subgrade, it can resist consolidation and movement, eliminating rutting in all layers except the asphalt surface [11].

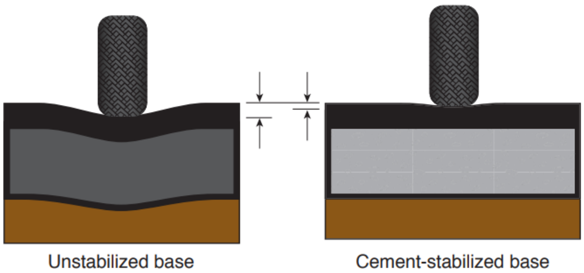

Figure 3-Rutting [11]

Although moisture infiltration can compromise unstabilized pavements, it is not valid for stabilized ones where cement binds the base, reducing permeability. Indeed, C.T.B. pavements provide a moisture-resistant base able to keep water out and maintain high levels of strength even when saturated, reducing the possibility for pumping of subgrade soil. [21]

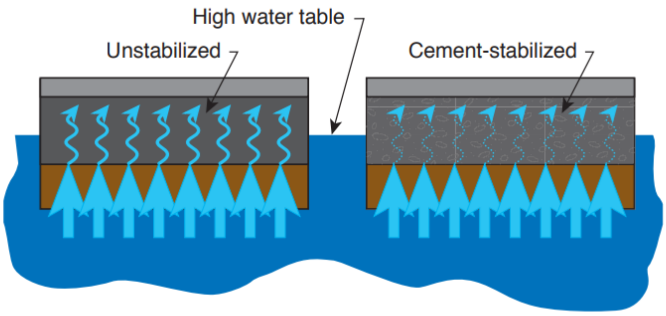

Figure 4-Moisture infiltration [11]

The cement-treated base material provides a durable, long-lasting base in all climates; it is also designed to resist damage caused by freeze and thaw cycles, rain, and spring-weather gaining strength with age even under traffic. [11-12]

CONSTITUENTS

1.1.1 Aggregates

Aggregates suitable for cement-bound granular mixture must comply with UNI EN 13242. They can be natural, artificial, recycled, or inert waste, appropriately pre-processed with physio-mechanical processes. [13][21]

The properties and the proper aggregates categories depend on the cement-bound granular mixture's position in the pavement structure and the traffic to be carried. Furthermore, aggregates must be volumetrically stable; otherwise, a laboratory evaluation of the mixture to check the performance is required. [13]

1.1.2 Cement

Cement shall be following UNI EN 197-1 and UNI EN 194-4. [13] [21]

Slow hardening cement has to be employed, with an initial setting time greater than 180 minutes and a strength class of 32,5 N. In exceptional cases, cement with strength class 42,5 N can also be used. [21]

The cement content depends on the aggregate material used but usually ranges from 2% to 4% in weight. Although any Portland cement can be employed, types I and II are most common. [12][21]

1.1.3 Water

Water shall be following UNI EN 1008. It shall not contain harmful impurities such as oil, acid, alkali, organic matter, clayey silt fractions, or any other detrimental substance that negatively affects the mixture's hardening and performance. [13] [21]

1.1.4 Additives

The additives are inorganic materials fine-milled which can be added to the bound granular mixture to modify its characteristics. They have to comply with the standard UNI EN 14227 (Cement bound granular mixtures). Instead, the additives usually required to obtain working times balanced with laying needs must follow UNI EN 934-2. [21]

SPECIFICATIONS

Table 1-Grading envelopes for granular mixtures [21]

Setacci ISO 3310 Dimensioni (mm)	**FUSO A Misto 0/31,5**	**FUSO B Misto 0/20 stretto**	**FUSO C Misto 0/20 ampio**
	Passante (%)		
40	100	-	-
31,5	80 - 100	100	100
20	65 – 85	85 – 100	85 – 100
16	53 - 70	-	-
10	40 – 55	55 – 80	55 – 84
6	30 - 42	42 – 66	42 – 72
2	18 - 30	23 – 43	23 – 50
0,40	8 - 18	10 – 24	10 – 30
0,18	6 - 14	6 – 16	6 – 20
0,063	5 - 10	4 - 9	4 - 11
Nota: Il fuso **B** è poco più ampio di A ed ha un minore contenuto di frazione grossa (la sua curva limite inferiore corrisponde a quella superiore di A nel campo della frazione grossa); si raccorda poi ad A nella parte della sabbia fine. Il fuso **C,** più ampio di B, ha la curva limite inferiore coincidente con quella del fuso **B.** La **curva limite inferiore** dei fusi **B** e **C** segue la legge di **Fuller** per **D = 31,5 mm**; inoltre attraversa il fuso A, restando tuttavia compresa all'interno di questo.			

According to new tender specifications, the granular mixture employed for manufacturing the cement bound has to have a particle size composition in one of the grading envelopes reported in Table 1. Moreover, cement content (usually between 2% and 4% in weight), water content, and additives must be expressed as a percentage by weight of total aggregates, and these percentages shall be determined by an accurate mix-design of the mixtures, as specified by B.U C.N.R. N.29, to meet the requirement reported in Table 2. [21]

Table 2-Requirements for cement bound mixtures [21]

Parametro	*Normativa*	*Valore*
Resistenza a compressione a 7gg	UNI EN 13286-41	$2,5 \leq R_c \leq 4,5$ MPa
Resistenza a trazione indiretta a 7gg	UNI EN 13286-42	$R_{ti} \geq 0,25$ MPa
Resistenza a trazione indiretta dopo 4 giorni di imbibizione, riferita al valore iniziale	UNI EN 13286-42	≥ 80%

In contrast to what is indicated in Table 2, in exceptional cases, compressive strengths can be accepted up to 7,5 MPa, but only if compatible with resistance requirements of the superstructure. [21]

ACCEPTANCE CONTROLS

The company has to submit the cemented bound mixtures for the acceptance of the Works Manager at least seven days before the beginning of works. Each mixture must be accompanied by the documentation of the formulation study carried out and compliance with performance requirements. Once the mix design has been accepted, it must be applied rigorously during the construction phases. However, in the granulometric curves, a margin of variation of ±5% for coarse aggregates and of ±2% for fine aggregates is admitted, whereas, for cement content, the admitted variation is ±0,5%. [21]

BLENDS PACKAGING

Cemented bound mixture has to be packed in an automated plant equipped with devices to ensure the uniformity of production and compliance with performance requirements. The storage area for aggregates has to be prepared to avoid harmful substances; moreover, the heaps must be separated. Furthermore, the refuelling operation must be carried out with the utmost care. Finally, cement and additives have to be protected against moisture and impurities. Deliveries on-site have to be accompanied by transport documents where the central plant, the construction site, the means of transport, and the mass of transported material are indicated. [21]

STABILISATION PROCESS

Aggregates are essential in pavement structures. However, good quality and suitable aggregates are not always available near the construction site; therefore, long distances are required. Nevertheless, in some cases, locally available aggregates can be employed despite the inferior quality using a process known as stabilization to modify their engineering properties and achieve requirements as a pavement material. The stabilization process includes many advantages:

- improves the stiffness and the tensile strength of materials;
- reduces pavement thickness;
- improves durability and resistance to water;
- reduces the swelling potential.

Furthermore, the stabilization mechanism can be distinguished into two categories: mechanical and chemical stabilization. Mechanical stabilization is based on compaction, mixing aggregates to improve gradation, and adding asphalt, aiming to coat the particles, impart adhesion, and help waterproof. Chemical stabilization, on the other hand, includes the addition of materials such as lime, cement, or fly-ash that react chemically with stabilized materials or react on their own to form cementing compounds. [6]

The effectivity to use in-situ and local marginal aggregates on or near the commercial paving site means avoiding the transportation of costly selected granular aggregates. Therefore, constructing a cement-treated base is often more economical than a granular one. Indeed granular borrow soil can provide an excellent material source, even requiring lower cement contents with respect to clay and silt soils. [8][14]

Material from failed flexible pavements can be salvaged economically by recycling and breaking them up, pulverizing, and stabilizing with a small quantity of Portland cement. The great advantage is that since approximately 90% of the material used is already in place, manipulation and transport costs are cut to a minimum. Moreover, old granular-base roads can be recycled into an excellent cement-treated base, even asphalt surfaces. [14]

REFLECTIVE CRACKS

Cracks develop for several reasons, and most of them represent a failure in the pavement, such as fatigue cracking or cracking due to base failure. However, other cracks, such as reflective cracks directly generated by cement-treated bases, generally do not reduce smoothness and serviceability. [15]

In particular, with the insertion of a stabilized base, fatigue cracking decreases due to its stiffness, and also vertical deflections and tensile strains in the asphalt surface are reduced. Moreover, base failures are reduced since stabilization helps keep moisture out of the base and improves material performance in saturated or freezing conditions. At the same time, subgrade failures are decreased thanks to the ability of the cement-treated base to spread traffic loads over wider areas. Nevertheless, cement-treated bases can source shrinkage cracks in the stabilized base layer, reflecting through the asphalt surface. [15]

These cracks are called "reflective cracks". They are not caused by structural deficiency but by a natural characteristic of cement stabilized bases. Therefore, cracks generation and spacing depend on material characteristics, construction procedure, and traffic loading. In particular, they are caused by shrinkage of the cement stabilized layer, which usually occurs early in the life of a pavement and results in movements that, being prevented by friction from underlying layers, cause tensions. Tensile strength on the cemented stabilized layer is limited, especially early; these tensions provoke cracks (Figure 5). [15][18]

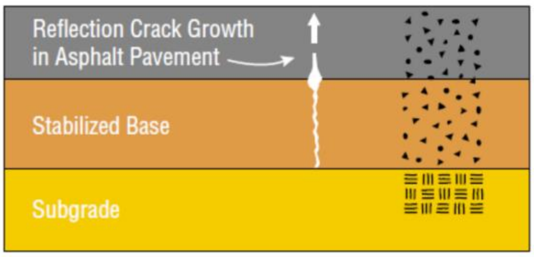

Figure 5 -Reflective cracks growth in asphalt pavement [21]

These cracks are mostly narrow, less than 3 mm; therefore, sufficient load transfer normally exists through aggregate interlock to keep pavement functioning. Instead, when wider cracks, greater than 6 mm, occur at the pavement surface, they can result in poor load transfer and increase stresses in the surface layers. It would lead to entire structure deterioration in the form of pumping of subgrade material, faulting the base, and increasing pavement roughness. Indeed, wide cracks have to be avoided. [15][17]

Figure 6-Example of reflective cracks [21]

Fortunately, there is the possibility of taking measures to minimize their occurrence since the causes and remedies for shrinkage have been under investigation for over 50 years. There are several preventative measures and design concepts that can be used to minimize this phenomenon and to reduce the possibility of reflection of cracks through the asphalt layer:

- appropriate construction techniques to provide reasonable quality control during field operations. Dealing with cement-treated bases, the quality of the project relies on essential factors, including the use of proper cement and water content, adequate compaction, and curing. Moreover, the stabilization process must be realized within two hours of cement mixing to guarantee that cement does hydrate before final compaction is achieved;
- compaction of the cement-treated base at slightly less water content than the optimum. An excessive drying, indeed, can lead to wide shrinkage cracks;
- reduction of the percentage of clay, because clay holds water and it is compacted at higher moisture content and generate the potential for shrinkage is more significant;

- the adequate proportion of the amount of cement in the mix. Enough cement should be added to achieve the desired engineering properties, but more than that is not required, not economical, and lead to additional cracking;
- use of admixtures such as shrinkage compensating cement, gypsum, water reducers, fly ash and ground granulated blast-furnace slag to reduce shrinkage potential. In particular, they reduce water demand, helping mixing process, extending mixing time, and for many granular soils, providing a filler material able to reduce the need for excess cement;
- provision of a stress relief layer in the pavement structure composed of flexible material interposed between the base and the surface layer;
- curing immediately after final compaction since the surface of the cement-treated base must be kept moist until a permanent moisture barrier is positioned and water trucks usually provide moisture to the pavement. Once the moisture barrier is placed, water curing can stop;
- delay of paving as long as practical following the placing of the prime coat. This delay allows more time for any shrinkage cracks to develop. Moreover, placing the surface after most of the shrinkage has occurred can result in fewer and thinner cracks;
- microcrack the pavement to reduce or eliminate reflection cracks. Loading application to the stabilized layer one to two days after final compaction introduces a network of closely spaced cracks that relieve shrinkage stresses and provide a crack pattern that minimizes wide cracks' development. Furthermore, since microcracking is performed early after placement, it does not impact the pavement's overall structural capacity as the cracks heal and the cemented layer gains strength with time. [15][17-19]

Other innovative techniques have been recently developed. A.Garcia-Hernández et al. (2020) demonstrated that encapsulated healing agents could delay the growth of reflective cracks in asphalt mixtures and postpone the asphalt surface's maintenance [23]. B. Evirgen, in 2021, investigated the utility of polyester-fibers-based soil geogrid as an alternative solution concerning the experimental performance analysis. [24]

FACTORS AFFECTING STRENGTH

In 1986, Draft THR13 stated that the bond strength is primarily influenced by the cement dosage, the type of aggregates, the density, the water content, and the curing conditions. Notably, they demonstrated that the strength increases more or less linearly with the increase of cement content. [41]

In 2016, Sounthararajah A. et al. found that tensile and compressive strength increase with the increase of cement dosage and curing period. In the same year, Nusit K. et al. demonstrated that the strength of these materials depends on water content at compaction and dry density. [35] [37]

In 2021 Songtao L. et al. found out that the curing periods greatly influence the strength and fatigue performance of cement-treated aggregate base materials [36].

ELASTIC MODULI

Despite several experimental studies available in the literature, there are still debates on the elastic modulus attributed to the cement-treated base material. Determining a suitable elastic modulus of C.T.B. material is challenging due to testing and interpreting the test results. For this reason, it is still preferable, for design intents, to use relationships between the strength and the modulus of elasticity instead of testing. [38]

For what concerns the use of relationships, many studies suggest correlations between the unconfined compressive strength [U.C.S.] and the Elastic Modulus [Ec].

In 1986, Thompson recommended using the normal concrete relationship provided by the American Concrete Institute [A.C.I.], where fc is the compressive strength in Mpa. [38]

$$Ec = 5000 \cdot \sqrt{fc}\ MPa$$

Equation 1- Concrete relationship, A.C.I.

In 1986, SANS Rules derived a different relationship, where σ_c is the unconfined compressive strength expressed in kPa. [40]

$$E_c = 4{,}16 \cdot {\sigma_c}^{0{,}88} + 3483\ MPa$$

Equation 2--Modulus of elasticity, Norme SANS- TRH13/1986

In 2003, Zollinger analysed the behavior of C.T.B. materials related to the advancement of strength and elastic Modulus under uniaxial compression. The Modulus of elasticity has been determined as the initial secant modulus at 25% of the ultimate stress. Notably, w is the mixture density in pcf, and $fc\ (t)$ is the compressive strength in psi at time t. [39]

$$Ec(t) = 4{,}38 \cdot w^{1{,}5} \cdot fc(t)^{0{,}75}\ psi$$

Equation 3-Modulus of elasticity, Zollinger

In 2004, Austroads provided a new equation: where UCS is the unconfined compressive strength expressed in MPa and k is a parameter between 1000 and 1250. [42]

$$E_c = k \cdot UCS\ MPa$$

Equation 4-Modulus of elasticity, Austroads 2004

Instead, it is possible to estimate the elastic modulus by interpreting test results. The stress-strain curvilinear relationship, derived from data analysis of the unconfined compressive and indirect tensile tests, gives the possibility to derive both tangent and secant moduli and the energy required to fracture the material (toughness).

2 EXPERIMENTAL PLAN

The primary purpose of this research work is to evaluate the variation of physical and mechanical properties of cement-treated base materials at the variation of some parameters such as the cement content, the water content, the lytic structure, and the compaction methodology. To achieve these objectives, a campaign of experimental tests is carried out in the Road Material Laboratory of the Polytechnic of Turin.

The material for testing has been provided by Sitalfa S.p.A., the company holding the concession for the highway "Torino-Bardonecchia," where the cement-treated base material is currently employed. The company, in addition, supplied the experimental analysis results carried out on its material by Tecnopiemonte S.p.A and the comparison with these was the starting point of the experimental plan.

Precisely, the experimental campaign has planned the following activities:

1) Material characterization, in terms of particle size distribution and theoretical maximum density;
2) Mix design of granular mixtures;
3) Proctor tests of granular mixtures to define the optimum water content and the maximum dry density;
4) Mix design of cement-bound mixtures, starting from granular mixtures and varying the cement content;
5) Proctor tests of cement-bound mixtures to define the optimum water content and the maximum dry density;
6) Realization of cement-bound samples by Proctor compaction;
7) Determination of indirect tensile strength and compressive strength;
8) Determination of elastic parameters by stress-strain curvilinear relationships.
9) Realization of cement-bound samples by Gyratory compaction;
10) Determination of indirect tensile strength;

MATERIAL CHARACTERIZATION

2.1.1 Sieves analysis

Figure 7-Aggregate material supplied by Sitalfa S.p.A.

The aggregate material supplied by the company consisted of three different particle size classes:

- coarse sand, with diameters from 0 to 8 mm;
- crushed stone, with diameters from 8 to 18 mm;
- crushed stone, with diameters from 18 to 30 mm.

The particle size distribution has been determined according to BS EN 933-1:2012 and included: washing, dividing, and separating the aggregate material classes into several particle size classifications of decreasing size through a series of sieves.

For what concerned the preparation of test portions, following EN 932-2, the size of each test portion should not be smaller than specified in Table 3.

Table 3-Minimum size of test portions, EN 933-1:2021

Upper aggregate size *D* mm	**Normal weight aggregates** kg	**Lightweight aggregates** litres
90	80	-
32	10	2,1
16	2,6	1,7
8	0,6	0,8
≤ 4	0,2	0,3

Washing and then dry sieving are necessary to determine the fine fraction accurately. Washing is performed in a 0,063 mm sieve with a guard sieve of 2 mm on the top, and the test portion is inserted on the top sieve, and it is washed until the water passing the 0,063 sieves is clear. Then the residue retained on the sieves is dried to constant mass at 105°C, and after cooling, the mass is recorded.

The granular distribution has been determined by selecting sieves according to the aggregate size. Particularly the 0,0063 mm sieve has been incorporated to take care of the fines that remained after washing. Then the washed and dried material is inserted in the sieving column (Figure 8) that is mechanically shaken.

Figure 8- Sieving column

In conclusion, the mass of particles retained on different sieves is then registered and expressed as a percentage of the original mass to calculate the cumulative percentage of the original mass passing each sieve.

2.1.2 Theoretical maximum density

The apparent density is calculated through the pycnometer method.

First, each pycnometer and the corresponding cap are weighted. Then the weights are registered, and two pycnometers are filled for 1/3 with the material. Then the material is left immersed in distilled and deaerated water for at least 4 hours, letting the water fill the voids (Figure 9).

Figure 9-Pycnometers, crushed stone 8/18

After the air extraction, pycnometers are filled up to the top with already deaerated water. As a result, a second weight and the water temperature measurement are registered.

In conclusion, the theoretical maximum density is calculated according to Equation 5.

$$TMD = \frac{m_c}{m_c - m_w - m_{wc+w}} \cdot \gamma_w$$

Equation 5-Theoretical maximum density

Table 4-Theoretical maximum density results

Aggregate material	TMD (g/cm3)
Coarse sand 0/8	2,728
Crushed stone 8/18	2,743
Crushed stone 18/30	2,740

Methodology

The experimental plan has involved using various types of machinery inside the Road Material Laboratory of the Polytechnic of Turin.

Specifically:

-Modified Proctor test apparatus;

-Gyratory compaction apparatus;

-Unconfined compression tester;

-Indirect tensile tester.

These types of machinery and their usages and objectives are explained below.

2.1.3 Modified Proctor test apparatus

Figure 10-Proctor test apparatus

The determination of the relationship between water content and dry density of hydraulically bound or unbound mixtures after compaction is performed using the Modified Proctor compaction test. Moreover, this test method is performed following BS EN 13286-2:2010.

The mixture is compacted in a specific mould (150x120). The compaction is performed by layers, specifically for each of the five layers by 56 blows of a falling rammer. Moreover, the rammer is characterized by a mass of 4,5 kg and a base diameter of 50 mm.

The test's objective is to define the optimum water content related to the maximum degree of compaction. Therefore, the results are reported in a graph in terms of water content and dry density. The peak of the results would represent the maximum achievable dry density.

2.1.4 Gyratory compaction apparatus

According to EN 12697-31:2019, the mixture is inserted in a cylindrical mould. The compaction is achieved by the concomitant action of low static compression and the shearing action resulting from the motion of the axis of the sample, which generates a conical surface of revolution, of apex O and 2φ angle at the apex. At the same time, the ends of the test piece should ideally remain perpendicular to the axis of the conical surface (Figure 16). Moreover, the machine allows fixing the number of gyrations or setting a fixed target height of the sample.

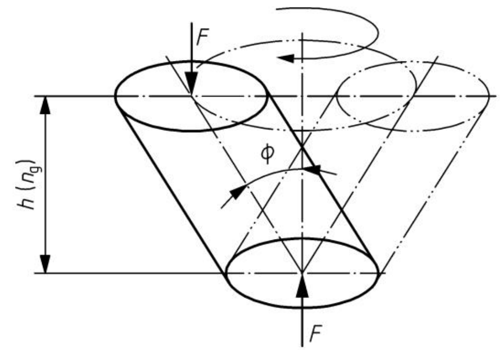

Key

F	axial resultant force
$h\ (n_g)$	height of specimen after a number of gyrations
ϕ	angle

Figure 11-Test piece motion diagram, EN 12697-31:2019

Figure 12-Gyratory compactor

2.1.5 Unconfined compression tester

Compressive strength for hydraulically bound mixtures (U.C.S.) is determined according to BS EN 13286-41:2003.

Cylindrical specimens (150x120) have been subjected to the test. A load is applied continuously and uniformly without shock, and the maximum force reached before failure must be recorded.

The apparatus used to perform the test comprises two parallel plates, one fixed and one moving horizontally, the load cell, and the strain transducer.

As specified in the rules, it is fundamental to guarantee the rupture of the specimen between 30 and 60 seconds of loading. Therefore, after some attempts, a loading rate of 0,2 mm/s has been set for the tests. For what concerns the results, the compressive strength has been obtained from Equation 6:

$$Rc = \frac{F}{Ac}$$

Equation 6- Compressive strength

Where:

-Rc is the compressive strength of the specimen of hydraulically bound mixtures expressed in $\frac{N}{mm^2}$;

-F is the maximum force reached before failure of the specimen expressed in N;

-Ac is the cross-section area of the specimen expressed in mm^2.

Figure 13- Unconfined compression tester

Figure 14- Unconfined compression tester, positioning of the sample

2.1.6 Indirect tensile tester

The indirect tensile strength for hydraulically bound mixtures (I.T.S.) has been determined according to BS EN 13286-42:2003.

Cylindrical specimens (150x120) have been subjected to a compression force applied along the two opposite generatrix until failure (Figure 15). It is fundamental that the compression machine achieves contact and applies the load continuously and uniformly without shock to obtain a uniform increase in stress lower than 0,2 $\frac{MPa}{s}$.

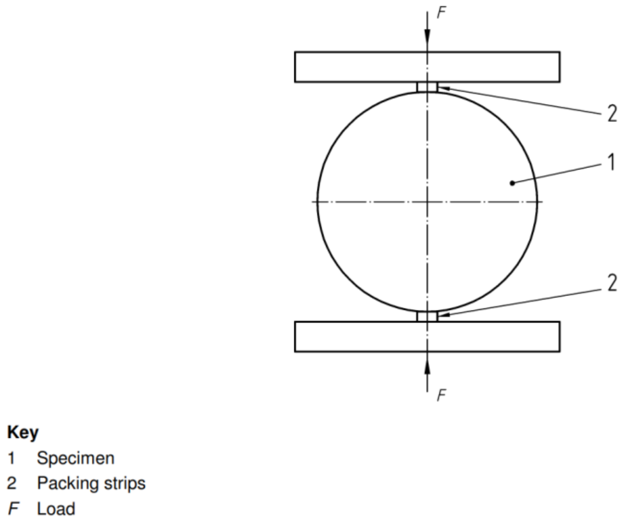

Figure 15-Principle of indirect tensile test, EN 13286-42_2003

The apparatus comprises the piston, the plate where the cylindrical sample is positioned, the load cell, and the strain transducer. The sample is supported by two packing strips made of wood, and it is inserted in a castle that allows its correct fastening during the loading phase (Figure 16-17). Moreover, the piston remains fixed during the test, whereas the bottom plate moves upwards until failure.

The indirect tensile strength has been therefore calculated from the maximum force reached before failure, and it is obtained from Equation 7:

$$R_{it} = \frac{2F}{\pi HD}$$

Equation 7-Indirect tensile strength

Where:

-R_{it} is the indirect tensile strength expressed in MPa;

- F is the force of failure expressed in N;

-H is the length of the specimen expressed in mm;

-D is the diameter of the specimen expressed in mm.

Moreover, the indirect tensile strength has to be expressed to the nearest 0,01 $\frac{N}{mm^2}$.

Figure 16- ITS test, lateral configuration of the indirect tensile tester

Figure 17 - ITS test, frontal configuration of indirect tensile tester

3 EXPERIMENTAL RESULTS

SIEVES ANALYSIS

Table 5- Test portions for aggregate size classification

Aggregate class	Test portions
Coarse sand 0/8	0,6 kg
Crushed stone 8/18	2,6 kg
Crushed stone 18/30	10 kg

Table 6-Sieves analysis results

	Coarse Sand 0/8	*Crushed Stone 8/18*	*Crushed Stone 18/30*
Sieve opening (mm)	Passing (%)	Passing (%)	Passing (%)
31,5	100,00	100,00	100,00
22,4	100,00	100,00	99,07
20	100,00	100,00	88,70
16	100,00	99,52	33,09
12,5	100,00	72,33	2,24
11,2	100,00	51,40	0,69
10	100,00	30,40	0,27
8	99,93	8,83	0,25
6,3	97,60	1,08	0,22
5,6	93,47	0,43	0,22
4	79,29	0,26	0,21
2	55,36	0,19	0,19
0,5	16,93	0,09	0,11
0,25	5,30	0,06	0,07
0,063	0,07	0,01	0,01

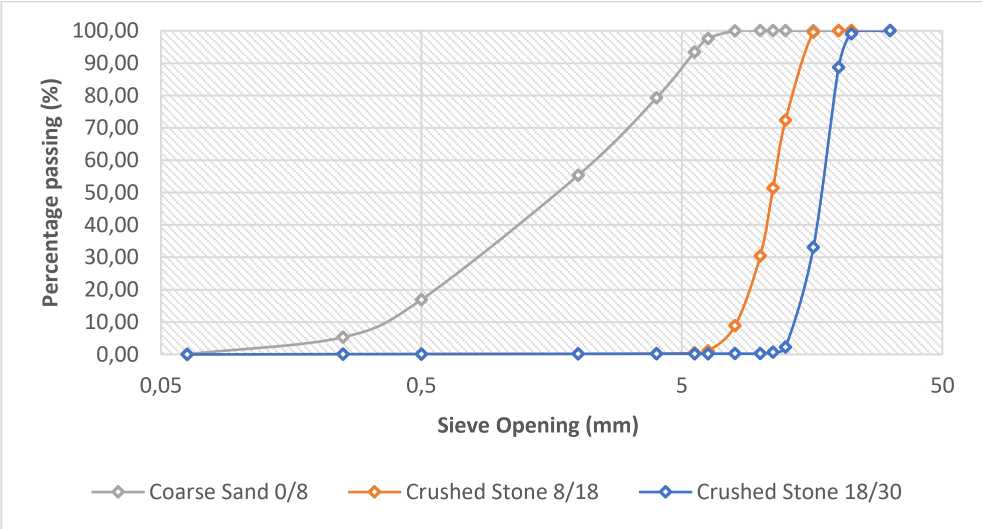

Figure 18- Grading curve

As mentioned above, the material characterization, already performed by Tecnopiemonte S.p.A., was available. Therefore, it is here reported just for completeness.

The sieve analysis performed by the company followed the UNI CEN ISO/TS 17892-12, which included both circular and squared grid sieves. Therefore, for easier comparison between the two analyses results, in Table 7, all circular sieves openings have been converted into squared ones.

Table 7- Sieve analysis, Tecnopiemonte S.p.A.

	Coarse Sand 0/8	*Crushed Stone 8/18*	*Crushed Stone 18/30*
Sieve opening (mm)	Passing (%)	Passing (%)	Passing (%)
31,5	100,0	100,0	99,0
24	100,0	100,0	90,1
20	100,0	100,0	61,0
12	100,0	79,0	0,0
8	100,0	14,0	0,0
4	80,0	0,0	0,0
2	57,0	0,0	0,0
0,4	19,0	0,0	0,0
0,18	8,5	0,0	0,0
0,075	3,1	0,0	0,0

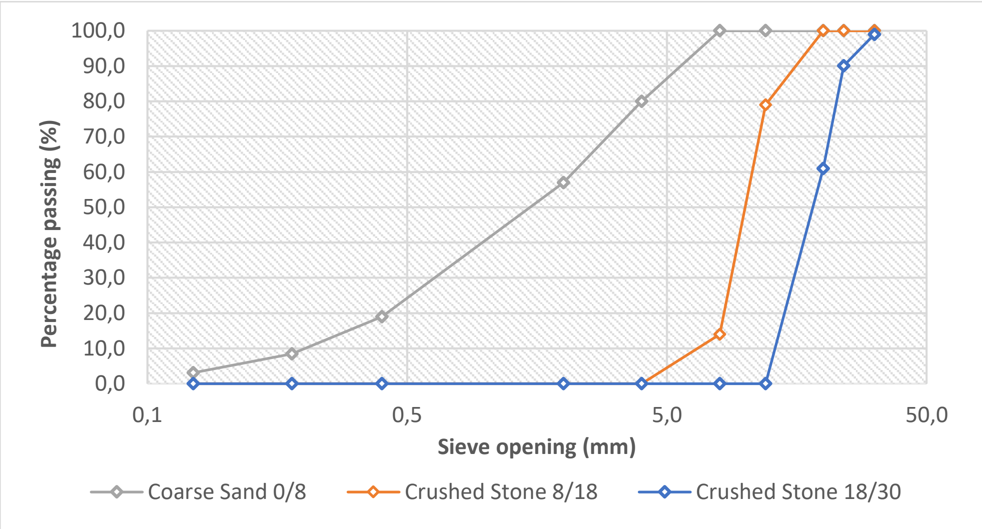

Figure 19- Grading curve, Tecnopiemonte S.p.A.

GRANULAR MIXTURES

Four different granular mixtures have been designed. The first two, GM1 and GM2, were made combining the three aggregate classes supplied by the company (0/8, 8/18, and 18/30 mm), whereas the other two, GM3 and GM4, were optimized by the addition of a fine fraction.

Table 8- Granular mixtures

Granular mixtures	Characteristics
GM1	Mix design according to a granular size distribution as much similar as possible to the granular mixture currently employed by Sitalfa S.p.A.
GM2	Mix design according to the "Città Metropolitana di Torino" grading envelope
GM3	Mix design according to the "Città Metropolitana di Torino" grading envelope, including $CaCO_3$ in the mixture.
GM4	Mix design according to the "Città Metropolitana di Torino" grading envelope, including Flowfill in the mixture.

3.1.1 Mix design

The four granular mixtures have adequately been designed with the support of the Excell "solver" command, useful for solving linear optimization problems.

Table 9-Granular mixture 1, Mix design

	Coarse sand (0/8)	*Crushed stone (8/18)*	*Crushed stone (18/30)*	*GM1*
Sieve opening (mm)	Passing (%)	Passing (%)	Passing (%)	Passing (%)
31,5	100,0	100,0	100,0	100,0
24	100,0	100,0	99,2	99,7
20	100,0	100,0	88,7	95,5
12	100,0	64,3	1,7	53,5
8	99,9	8,9	0,3	41,9
4	79,5	0,4	0,3	32,0
2	55,9	0,3	0,3	22,5
0,4	13,4	0,2	0,2	5,4
0,18	4,5	0,1	0,1	1,9
0,075	1,6	0,1	0,1	0,7
Percentages (%)	40	20	40	100

Table 10-Granular mixture 2, Mix design

	Coarse sand (0/8)	*Crushed stone (8/18)*	*Crushed stone (18/30)*	*GM2*
Sieve opening (mm)	Passing (%)	Passing (%)	Passing (%)	Passing (%)
31,5	100,0	100,0	100,0	100,0
24	100,0	100,0	99,3	99,7
20	100,0	100,0	88,7	96,1
12	100,0	64,6	1,7	58,7
8	99,9	8,9	0,3	47,2
4	100,0	0,4	0,3	36,3
2	55,9	0,3	0,3	25,5
0,4	14,3	0,2	0,2	6,6
0,18	5,3	0,2	0,1	2,5
0,075	2,0	0,1	0,1	1,0
Percentage (%)	45	20	35	100

Table 11- GM1 VS. GM2

Aggregate material	**GM1**	**GM2**
Coarse sand 0/8	40%	45%
Crushed stone 8/18	20%	20%
Crushed stone 18/30	40%	35%

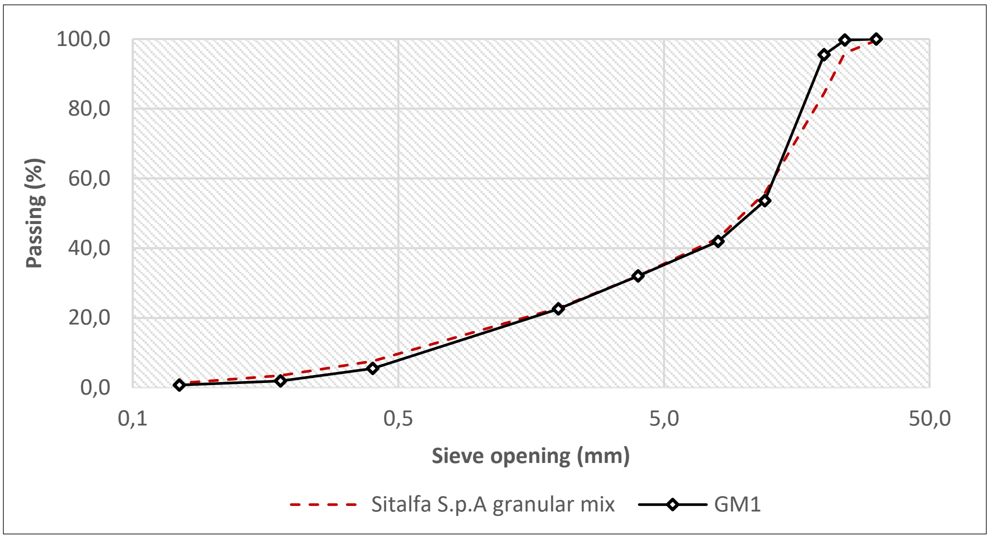

Figure 20-GM1 vs Sitalfa S.p.A granular mix

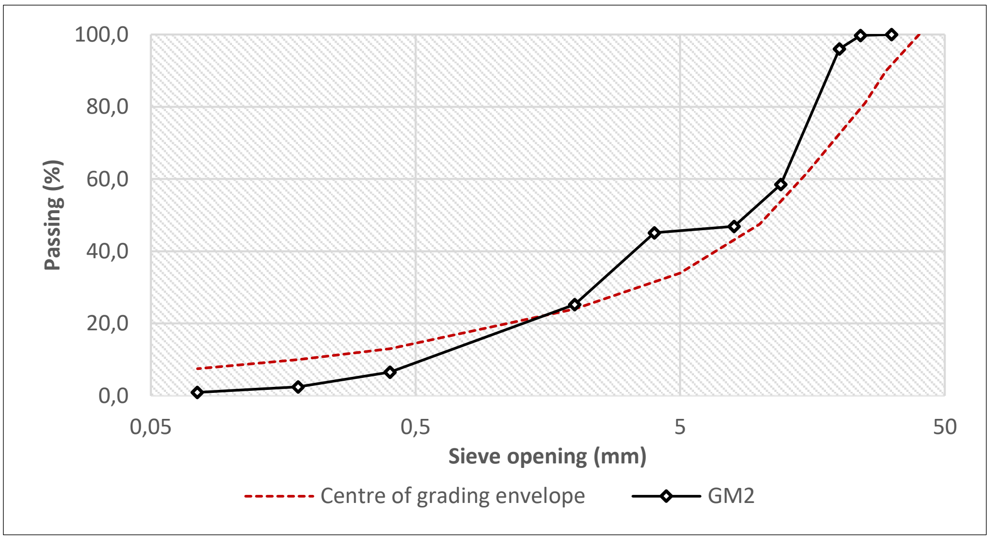

Figure 21-GM2 vs.Centre of grading envelope "Citta Metropolitana di Torino"

A direct comparison between GM1 and GM2 is inevitable; therefore, it is worth remembering the difference between the two. GM1 has been designed to obtain the exact curve of the mixture currently used by Sitalfa S.p.A., which was itself designed according to the grading envelope "Città Metropolitana di Torino" (Figure 20). Instead, GM2 has just been designed to respect the grading envelope (Figure 21).

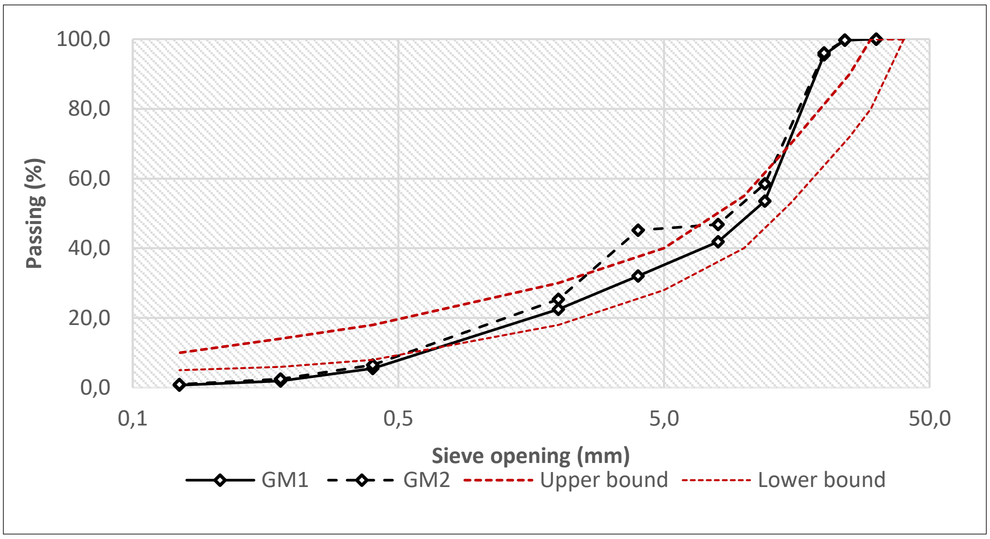

Figure 22- GM1 vs. GM2

In figure 22, the two grading curves have been reported together. Regarding the difference between the two, they are quite similar at the top and at the bottom, but 5 percentage points more of coarse sand 0/8 let the GM2 curve significantly rise in the central part. However, the main issue that concerns both of them is an evident lack of fine fraction, graphically visible since the tails of the curves are lower than the grading envelope. From this observation, it has been decided to design the other two granular mixtures. Indeed, the addition of a fine fraction has been taken into account for GM3 and GM4.

Table 12- Granular mixture 3, Mix design

Sieve opening (mm)	*Coarse sand (0/8)*	*Crushed stone (8/18)*	*Crushed stone (18/30)*	*Filler (CaCO3)*	*GM3*
31,5	100,0	100,0	100,0	100,0	100,0
24	100,0	100,0	98,2	100,0	99,4
20	100,0	100,0	86,4	100,0	95,5
12	100,0	64,5	1,7	100,0	58,5
8	100,0	8,8	0,1	100,0	44,2
4	84,0	0,3	0,1	100,0	36,6
2	57,5	0,2	0,1	100,0	27,5
0,4	13,0	0,2	0,1	99,2	12,2
0,18	3,9	0,2	0,1	97,1	8,9
0,075	0,7	0,1	0,0	92,3	7,4
Percentages (%)	34	25	33	8	100

Table 13- Granular mixture 4, Mix design

Sieve opening (mm)	Coarse sand (0-8)	Crushed stone (8-18)	Crushed stone (18-30)	Filler (FLOWFILL)	GM4
31,5	100,0	100,0	100,0	100,0	100,0
24	100,0	100,0	98,2	100,0	99,4
20	100,0	100,0	86,4	100,0	95,5
12	100,0	64,5	1,7	100,0	58,5
8	100,0	8,8	0,1	100,0	44,3
4	84,0	0,2	0,1	100,0	36,6
2	57,5	0,2	0,1	100,0	27,4
0,4	12,9	0,1	0,1	99,9	12,0
0,18	3,9	0,0	0,0	99,6	8,8
0,075	0,7	0,0	0,0	98,7	7,6
Percentages (%)	34,5	25	33	7,5	100

Table 14-GM3 VS. GM4

Aggregate material	GM3	GM4
Coarse sand 0/8	34%	34,5%
Crushed stone 8/18	25%	25%
Crushed stone 18/30	33%	33%
CaCO3	8%	7,5%

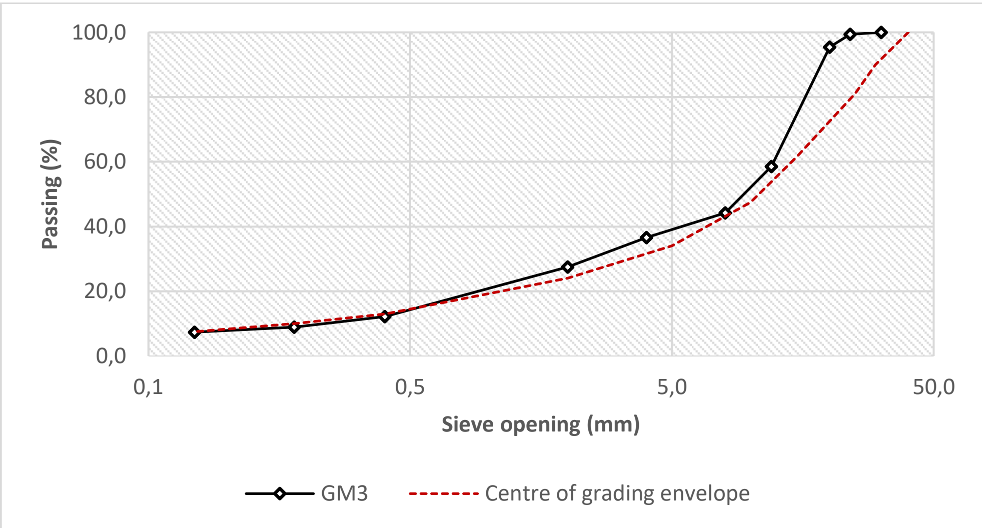

Figure 23-GM3 vs. Grading envelope

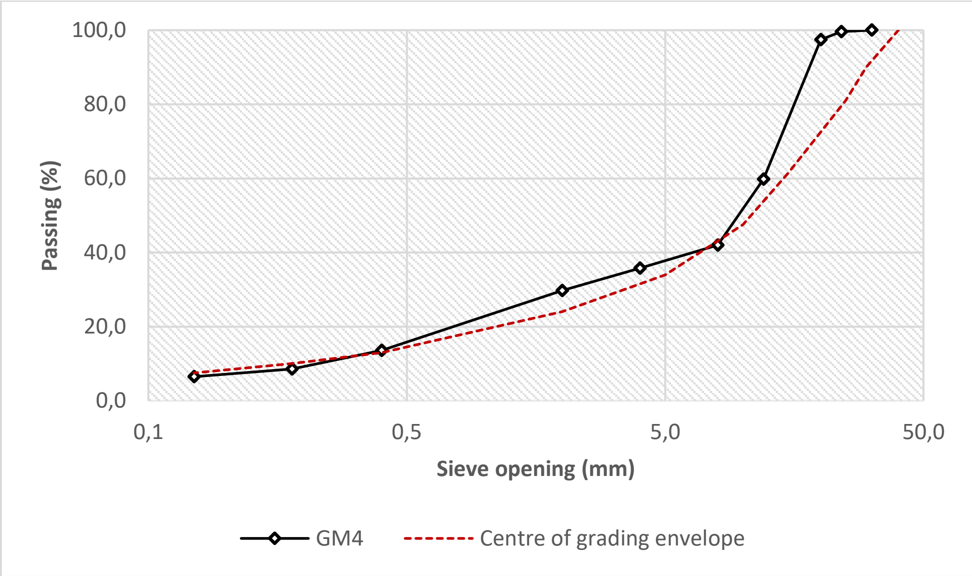

Figure 24- GM4 vs. Grading envelope

As already mentioned, GM3 and GM4 have been designed starting from the necessity of an additional fine fraction in granular mixtures to respect the grading envelope in the tail of the curves.

GM3 contained $CaCO_3$ as the missing fine fraction (Figure 23). However, this filler has yielded bad results since it almost seemed hydrophobic, and this caused a complex blending. Therefore, GM4 has been designed including a substitute filler (FLOWFILL), obtained from the milling of carbonate rocks (Figure 23).

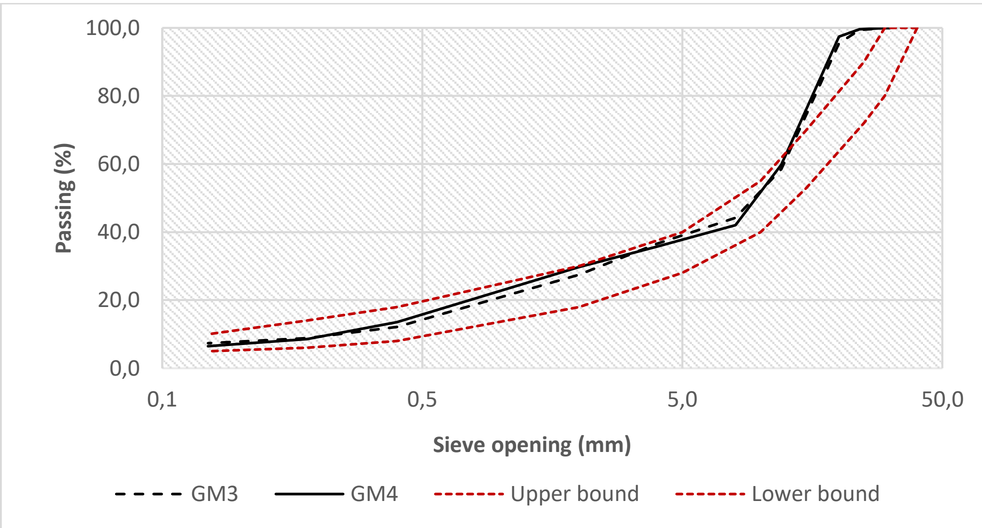

Figure 25-GM3 vs. GM4

Moreover, as expected, the addition of these fine fractions translates into a raise of the tails of the curves (Figure 25). The two granular mixtures are totally comprised within the grading envelope regarding the fine fraction.

3.1.2 Proctor tests

Modified Proctor tests have been performed on all the designed granular mixtures, as indicated in chapter 3.1.3, and the results of the four proctor tests have been collected in Tables 15-18. The displayed initial water content is the percentage of water initially included in the mixture, but for several reasons, a small part of the water is lost during the tests; therefore, the measured one, which is also indicated, is lower.

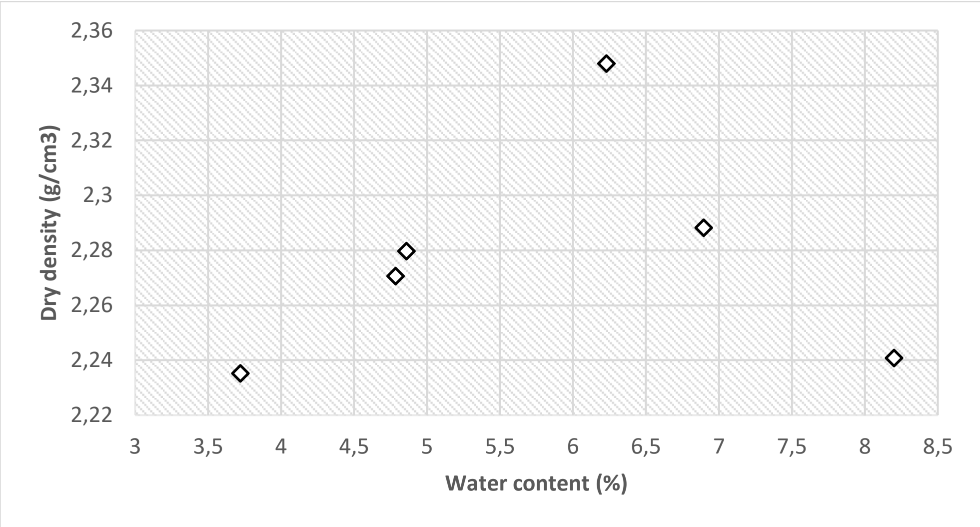

Figure 26-GM1, Proctor bell

Table 15-GM1, Proctor test results

Dry density	w	w in
[g/cm3]	%	%
2,235	3,72	4
2,271	4,79	5
2,280	4,86	6
2,348	6,23	7
2,288	6,90	8
2,241	8,20	9

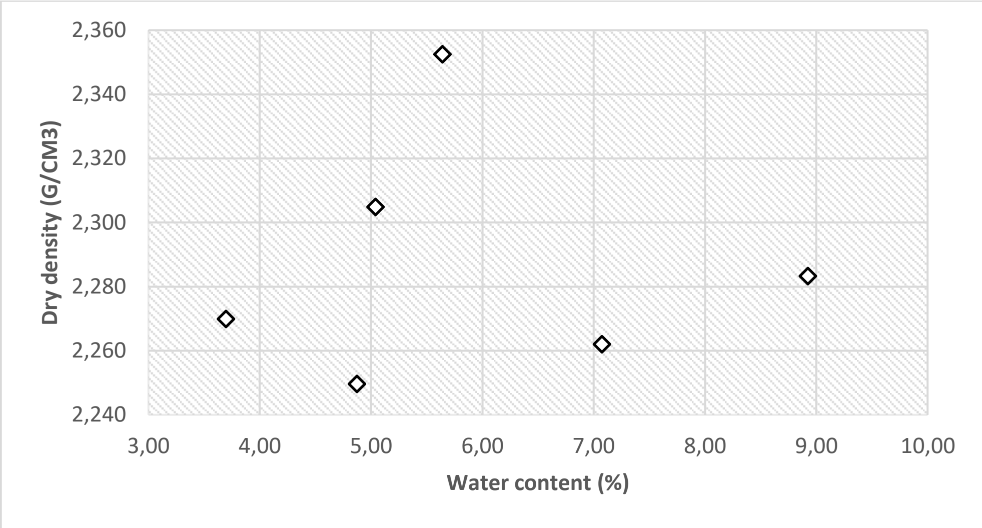

Figure 27-GM2, Proctor bell

Table 16-GM2, Proctor test results

Dry density	w	w in
[g/cm3]	%	%
2,270	3,70	4
2,250	4,87	5
2,305	5,04	6
2,352	5,64	7
2,262	7,07	8
2,283	8,93	10

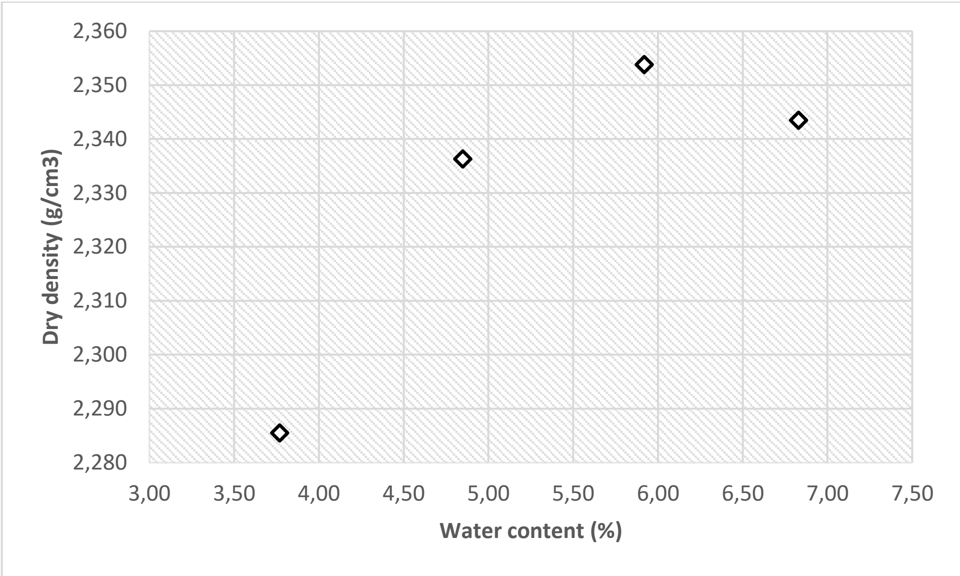

Figure 28- GM3, Proctor bell

Table 17-GM3, Proctor test results

Dry density	w	w in
[g/cm3]	%	%
2,285	3,77	4
2,336	4,85	5
2,354	5,92	6
2,343	6,83	8

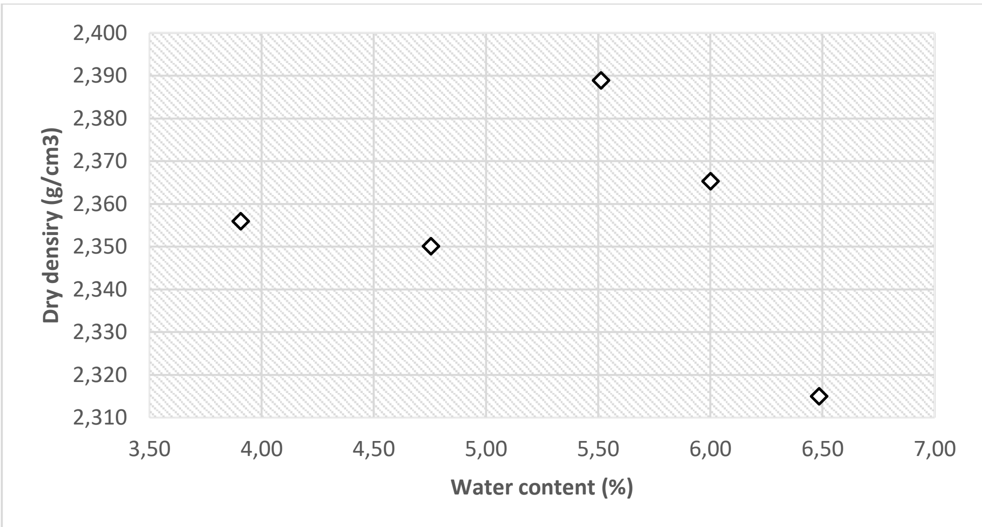

Figure 29-GM4, Proctor bell

Table 18-GM4, Proctor test results

Dry density	w	w in
[g/cm3]	%	%
2,356	3,91	4
2,350	4,76	5
2,389	5,51	6
2,365	6,00	7
2,315	6,49	8

In conclusion, the peaks in the Proctor bell graphs would represent the maximum degree of compaction and the optimum water content. These results are collected in Table 19, and it is noticeable that the optimum water content is close to 6% for all the mixtures.

Table 19-GM, Proctor tests results

Granular mixture	Optimum Water content (%)	Dry density (g/cm3)
GM1	5,64	2,352
GM2	6,23	2,348
GM3	5,92	2,354
GM4	5,51	2,389

CEMENT-BOUND MIXTURES

Two cement-bound mixtures, CBM1 and CBM4, have been designed to evaluate the influence of cement dosage. In particular, these two mixtures start respectively from GM1 and GM4. The choice has been thought: GM1 is selected to compare the results with the one obtained by Tecnopiemonte S.p.A., whereas GM4 for the influence of the mineral filler.

Different dosages of cement, ranging from 1,5% to 3,5%, are investigated to define the minimum dosage for CBM1 and CBM4 to comply with reference standards.

Table 20- CBM1

CBM1	GM	CEMENT CONTENT
CBM1.2,0	GM1	2,0%
CBM1.2,5	GM1	2,5%
CBM1.3,0	GM1	3,0%
CBM1.3,5	GM1	3,5%

Table 21-CBM1.2,0, Test portions

Material	CBM1.2,0	CBM1.2,5	CBM1.3,0	CBM1.3,5
Coarse sand 0/8	40%	40%	40%	40%
Crushed stone 8/18	20%	20%	20%	20%
Crushed stone 18/30	40%	40%	40%	40%
Cement	2,0%	2,5%	3,0%	3,5%

Table 22-CBM4

CBM4	GM	CEMENT CONTENT
CBM4.1,5	GM4	1,5%
CBM4.2,0	GM4	2,0%

Table 23-CBM4.1,5, Test portions

Material	CBM4.1,5	CBM4.2,0
Coarse sand 0/8	34,5%	34,5%
Crushed stone 8/18	25%	25%
Crushed stone 18/30	33%	33%
FLOWFILL	7,5%	7,5%
Cement	1,5%	2,0 %

3.1.3 Proctor tests

A Proctor study has been performed as indicated in chapter 3.1.3 to define the optimum water content and the maximum dry density for the cemented mixtures. Unlike the granular mixtures, it was impossible to estimate the final water content because of the hydration of cement; indeed, only the initial water content is indicated.

3.1.3.1 CBM1

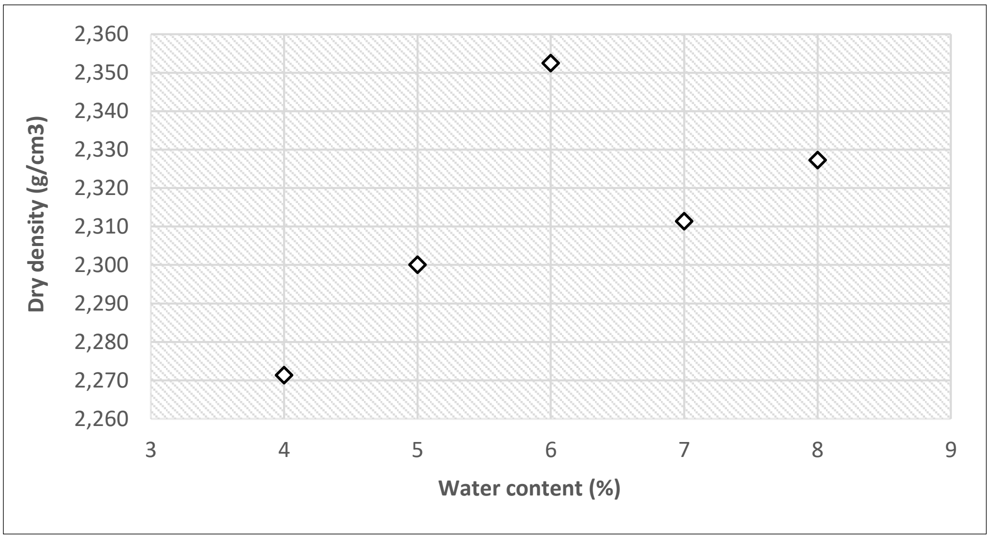

Figure 30-CBM1.2,5,Proctor bell

Table 24-CBM1.2,5, Proctor test results

Dry density	**Water content**
[g/cm3]	**[%]**
2,271	4
2,300	5
2,352	6
2,311	7
2,327	8

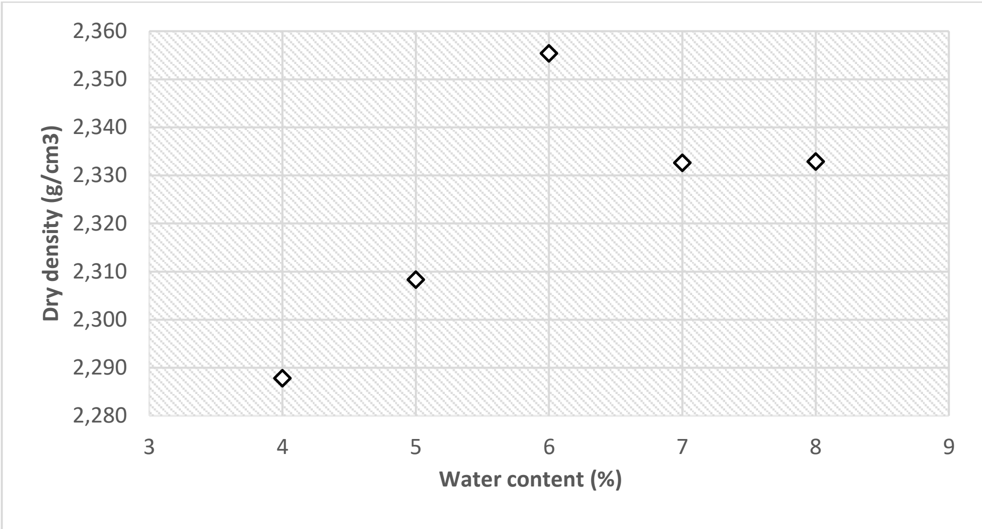

Figure 31-CBM1.3,0, Proctor bell

Table 25-CBM1.3,0, Proctor test results

Dry density [g/cm3]	Water content [%]
2,288	4
2,308	5
2,355	6
2,333	7
2,333	8

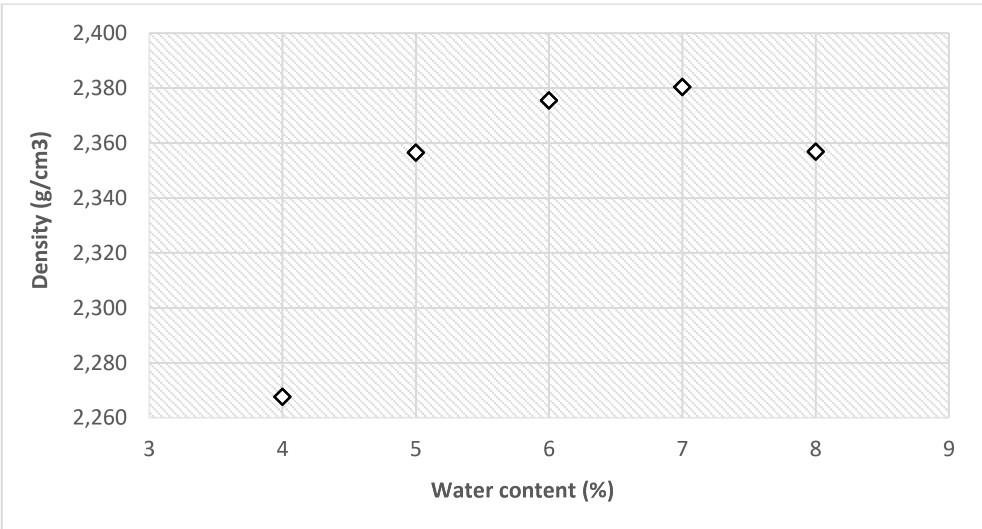

Figure 32-CBM1.3,5, Proctor bell

Table 26-CBM1.3,5, Proctor test results

Dry density [g/cm3]	Water content [%]
2,268	4
2,356	5
2,375	6
2,380	7
2,357	8

Proctor tests have been performed for all the cemented mixtures apart from CBM1.2,0, for which the optimum water content has been estimated since it is almost constant for low cement dosages.

In conclusion, the results of the tests are reported in Table 27, where the optimum water content and maximum density are indicated.

Table 27-CBM1, Proctor tests results

CBM	Dry density (g/cm3)	Optimum water content (%)
CBM1.2,0	-	6,00
CBM1.2,5	2,352	6,00
CBM1.3,0	2,355	6,00
CBM1.3,5	2,380	7,00

3.1.3.2 CBM4

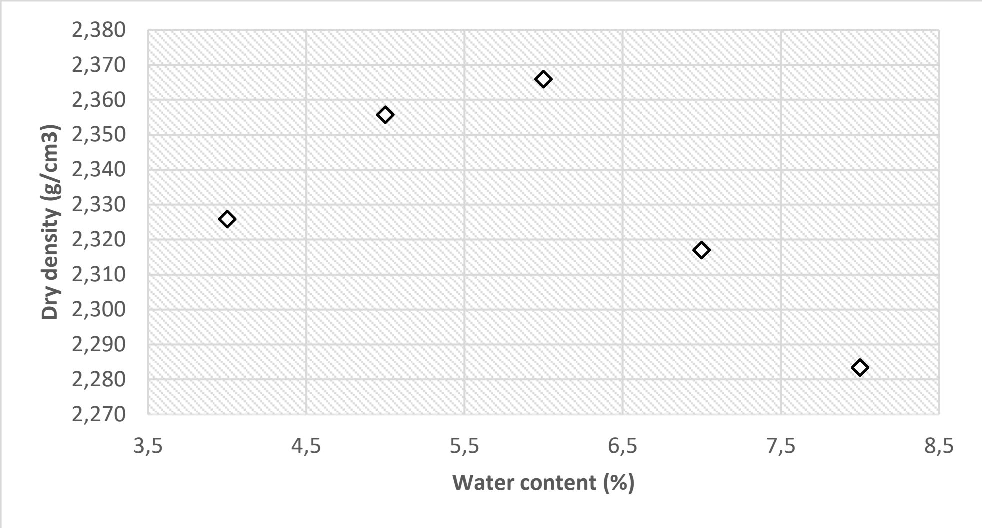

Figure 33-CBM4.1,5, Proctor bell

Table 28-CBM4.1,5, Proctor test results

Dry density	Water content
[g/cm3]	%
2,326	4
2,356	5
2,366	6
2,317	7
2,283	8

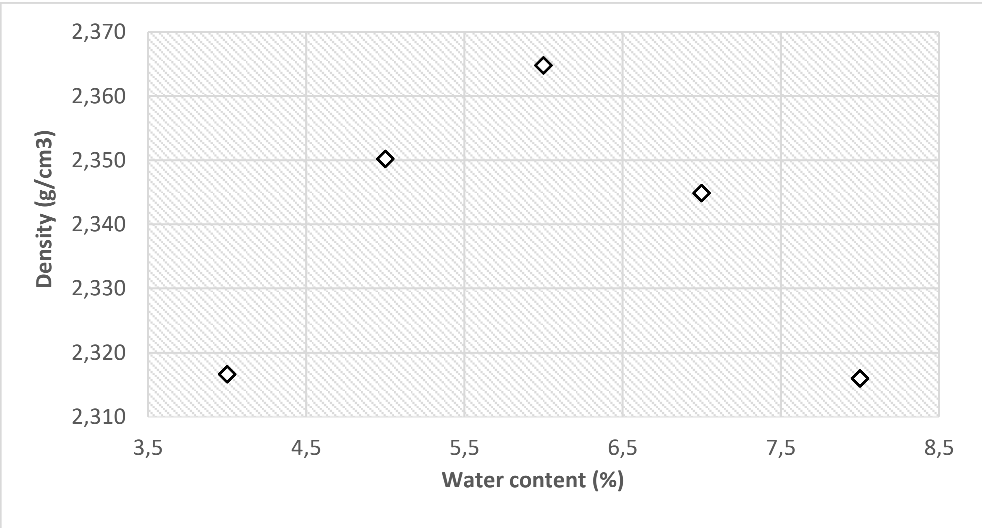

Figure 34-CBM4.2,0, Proctor bell

Table 29-CBM4.2,0, Proctor test results

Dry density	Water content
[g/cm3]	%
2,317	4,00
2,350	5,00
2,365	6,00
2,345	7,00
2,316	8,00

In this case, the optimum water content is constant and not affected by the slight increase in cement content. Therefore, the results of the tests are reported in Table 30, where the optimum water content and maximum density are indicated.

Table 30-CBM4, Proctor tests results

CBM	Dry density (g/cm3)	Optimum water content (%)
CBM4.1,5	2,366	6,00
CBM4.2,0	2,365	6,00

MECHANICAL PROPERTIES

Mechanical properties of cement-bound mixtures have been investigated by subjecting cylindrical samples 150x120 to specific tests. For the production of cylindrical specimens, the Proctor test apparatus is specified in the legislation. However, it has also been decided to use the Gyratory compaction apparatus to compare the results.

3.1.4 Proctor compaction

Table 31- CBM samples, Proctor compaction

CBM	OPTIMUM W (%)	DIMENSION (MM)	N°
CBM1.2,0	6%	150x120	6
CBM1.2,5	6%	150x120	6
CBM1.3,0	6%	150x120	6
CBM4.1,5	6%	150x120	6
CBM4.2,0	6%	150x120	6

Samples have been left for seven days in a humidity and temperature-controlled room to ensure a consistent moisture condition (95% humidity-20°C) (Figure 34). Remarkably, after the first 24 hours in the room, they have been extruded from the Proctor moulds and left curing for another six days. (Figures 35-36).

Figure 35-Controlled room

Figure 36-First 24H of curing in the controlled room

Figure 37-Curing in the controlled room

3.1.4.1 U.C.S tests

Three samples for each cement-bound mixture have been subjected to the unconfined compressive test as indicated in the legislation.

3.1.4.1.1 CBM1

Figure 38-CBM1.2,0, U.C.S. sample, Proctor compaction

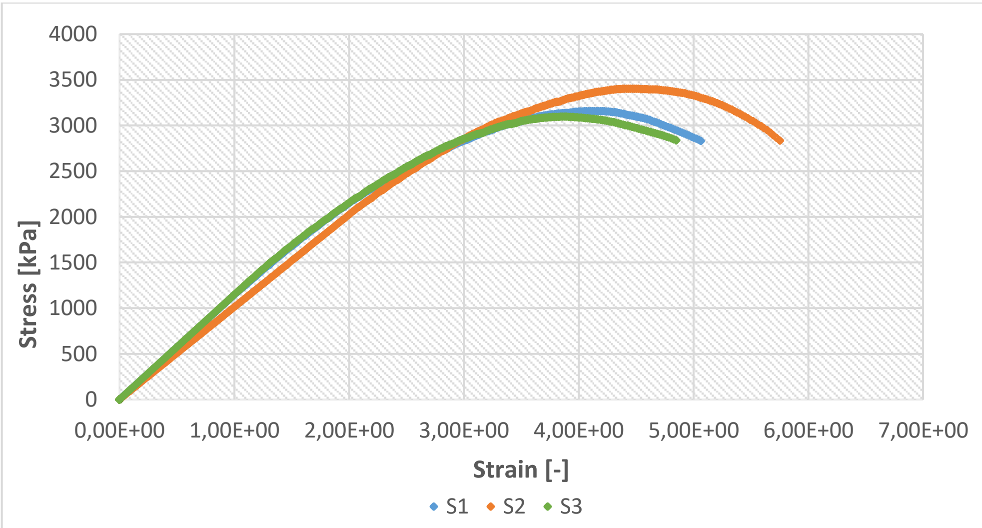

Figure 39-Stress-strain relationship,UCS,CBM1.2,0

Table 32-CBM1.2,0, U.C.S test results, Proctor compaction

CBM 1.2,0	Max Load (kN)	UCS (MPa)	UCS Average (MPa)	St. dev. (Mpa)
S1	55,77	3,16	3,22	0,16
S2	60,08	3,40		
S3	54,70	3,10		

Figure 40-CBM1.2,0,U.C.S. sample, Proctor compaction

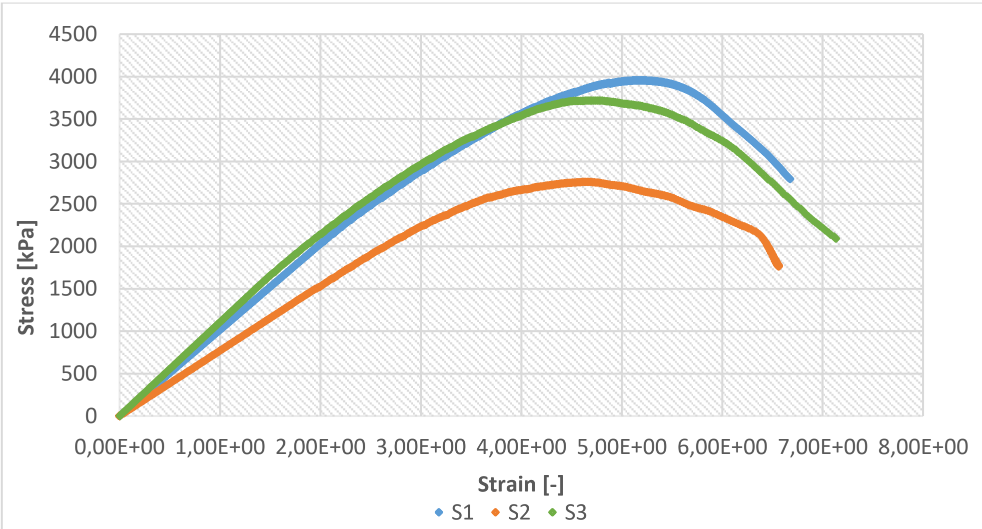

Figure 41-Stress-strain relationship,UCS,CBM1.2,5

Table 33-CBM1.2,5, U.C.S test results, Proctor compaction

CBM 1.2,5	Max Load (kN)	UCS (MPa)	UCS Average (MPa)	St. dev. (Mpa)
1	69,88	3,95		
2	48,73	2,76	3,84	0,17
3	65,70	3,72		

Since the second result of the UCS tests for CBM1.2,5 is very different from the others, it is considered an outlier and it has been deleted.

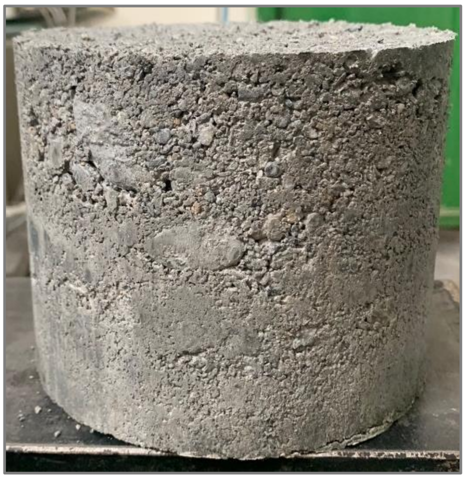

Figure 42-CBM1.3,0,U.C.S. sample, Proctor compaction

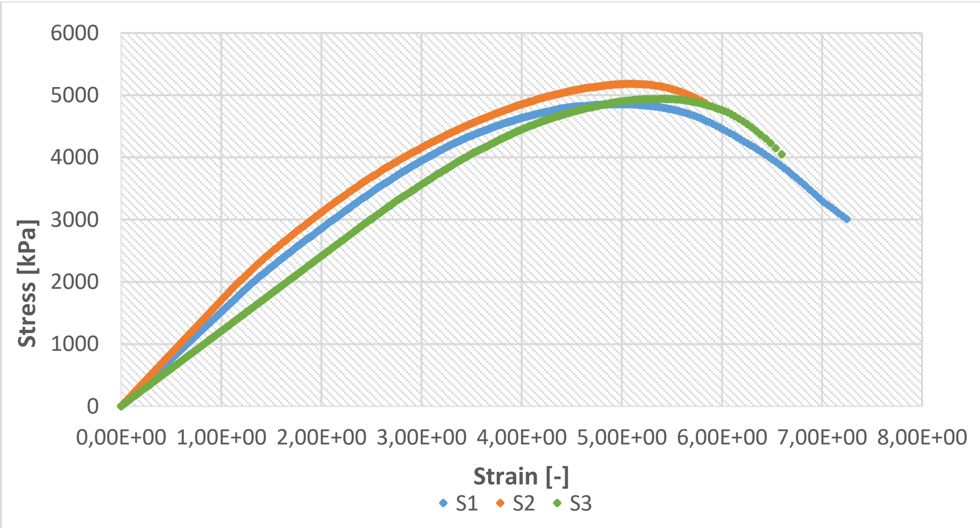

Figure 43-Stress-strain relationship,UCS,CBM1.3,0

Table 34-CBM1.3,0, U.C.S test results, Proctor compaction

CBM 1.3,0	Max Load (kN)	UCS (MPa)	UCS Average (MPa)	St. dev. (Mpa)
1	85,76	4,85	4,99	0,17
2	91,53	5,18		
3	87,26	4,94		

3.1.4.1.2 CBM4

Figure 44-CBM4.1,5,U.C.S. sample, Proctor compaction

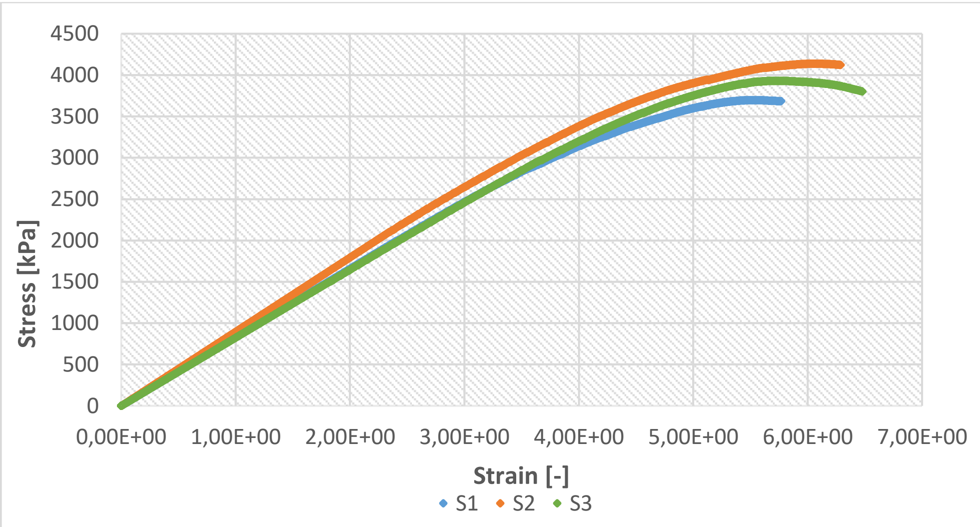

Figure 45-Stress-strain relationship,UCS,CBM4.1,5

Table 35-CBM4.1,5, U.C.S test results, Proctor compaction

CBM 4.1,5	Max Load (kN)	UCS (MPa)	UCS Average (MPa)	St. dev. (Mpa)
1	65,35	3,70	3,92	0,22
2	73,12	4,14		
3	69,47	3,93		

Figure 46-CBM4.2,0,U.C.S. sample, Proctor compaction

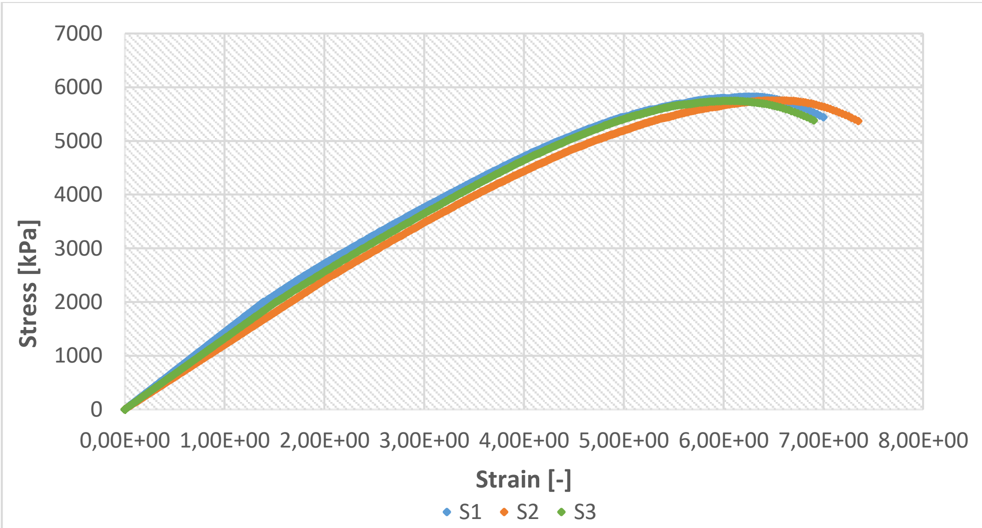

Figure 47-Stress-strain relationship,UCS,CBM4.2,0

Table 36-CBM4.2,0, U.C.S test results, Proctor compaction

CBM 4.2,0	Max Load (kN)	UCS (MPa)	UCS Average (MPa)	St. dev. (Mpa)
S1	102,87	5,82	5,77	0,04
S2	101,62	5,75		
S3	101,50	5,74		

According to the requirements of cement-bound mixtures presented in chapter 1, the UCS results have to be checked. The UCS value should be comprised between 2,5 MPa and 4,5 MPa, and in exceptional cases, this range can be extended to 7,5 MPa. About that, all the mixtures can be considered acceptable.

3.1.4.2 I.T.S. tests

Also, three samples for each cement-bound mixtures have been tested for the indirect tensile strength evaluation.

3.1.4.2.1 CBM1

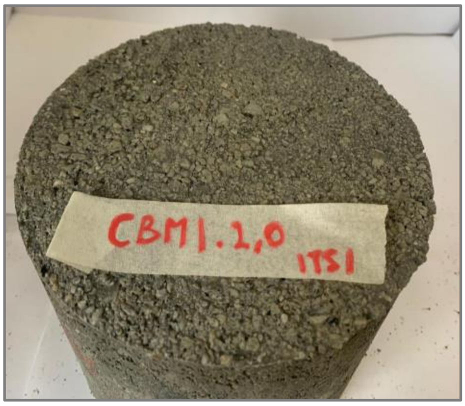

Figure 48-CBM1.2,0, I.T.S. sample, Proctor compaction

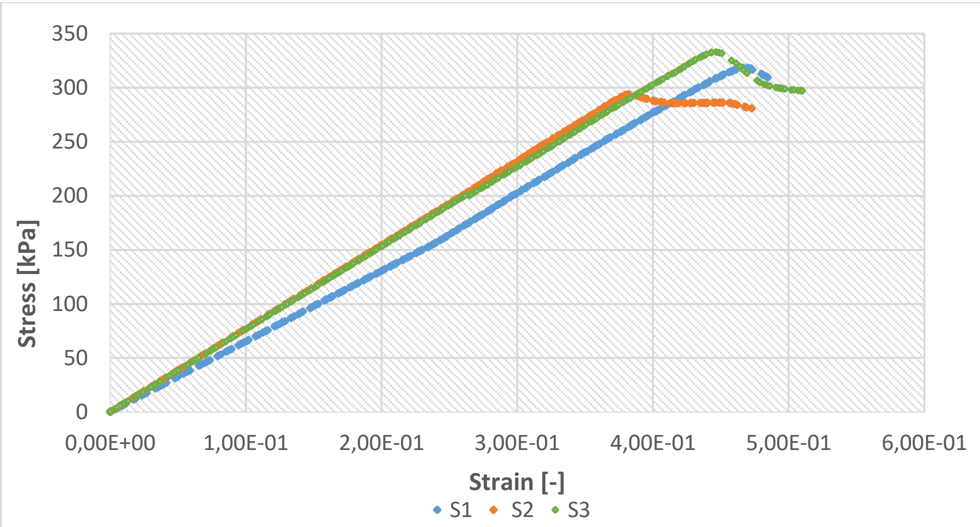

Figure 49-Stress-strain relationship, ITS, CBM1.2,0

Table 37- CBM1.2,0, results of ITS tests

CBM 1.2,0	Max Load (kN)	ITS (MPa)	ITS Average (MPa)	St. dev. (Mpa)
S1	5,63	0,20	0,20	0,01
S2	5,19	0,18		
S3	5,88	0,21		

Figure 50- CBM1.2,5, I.T.S. sample, Proctor compaction

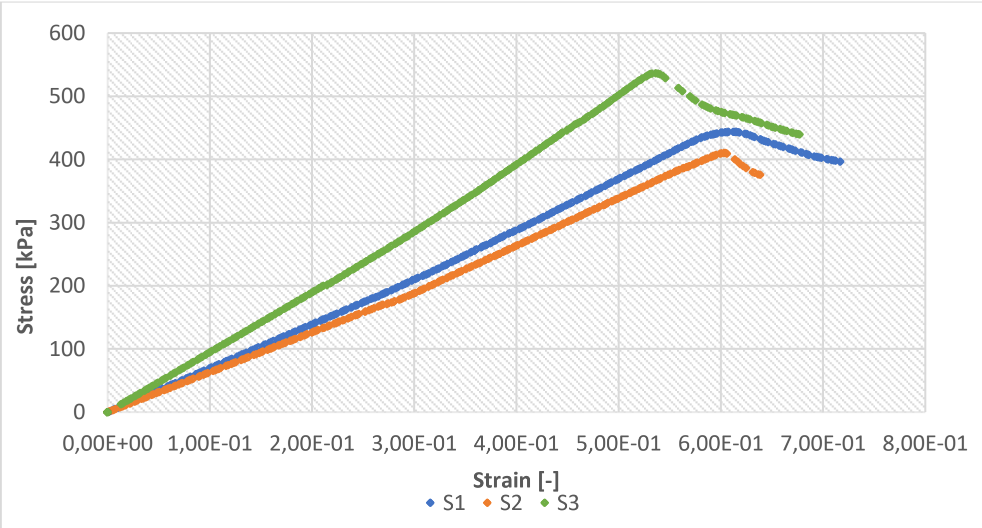

Figure 51-Stress-strain relationship,ITS,CBM1.2,5

Table 38-CBM1.2,5, results of ITS tests

CBM 1.2,5	Max Load (kN)	ITS (MPa)	ITS Average (MPa)	St. dev. (Mpa)
S1	7,843	0,28	0,29	0,04
S2	7,249	0,26		
S3	9,483	0,33		

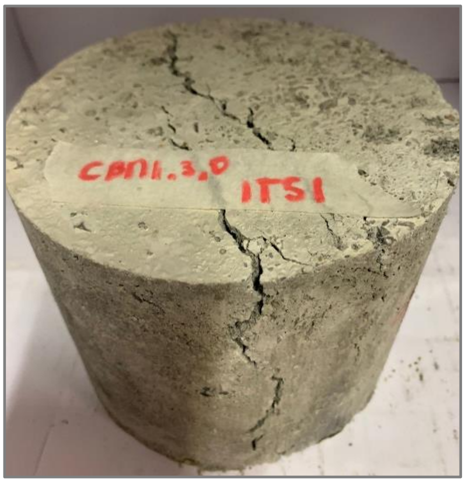

Figure 52-CBM1.3,0, I.T.S. sample, Proctor compaction

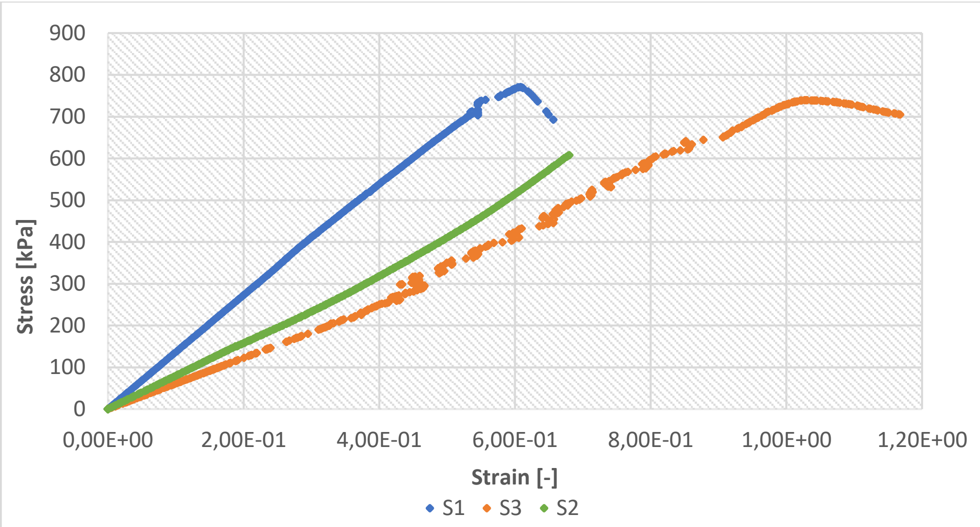

Figure 53-Stress-strain relationship,ITS,CBM1.3,0

Table 39-CBM1.3,0, results of ITS tests

CBM 1.3,0	Max Load (kN)	ITS (MPa)	ITS Average (MPa)	St. dev. (Mpa)
S1	13,62	0,48	0,44	0,05
S2	10,87	0,38		
S3	13,06	0,46		

3.1.4.2.2 CBM4

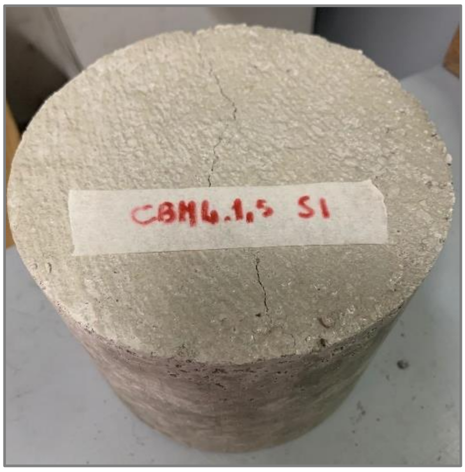

Figure 54-CBM4.1,5, I.T.S. sample, Proctor compaction

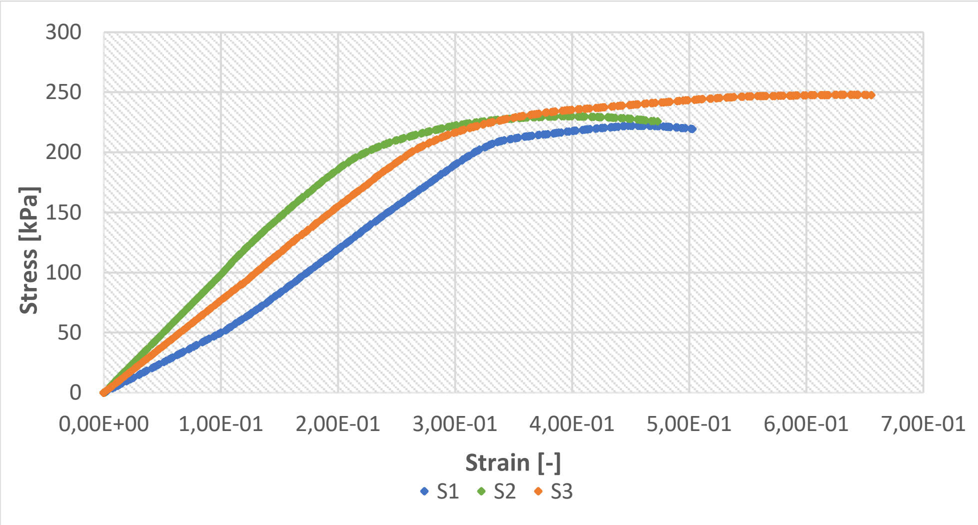

Figure 55-Stress-strain relationship,ITS,CBM4.1,5

Table 40-CBM4.1,5, results of ITS tests

CBM 4.1,5	Max Load (kN)	ITS (MPa)	ITS Average (MPa)	St. dev. (Mpa)
S1	3,93	0,14	0,15	0,01
S2	4,07	0,14		
S3	4,38	0,15		

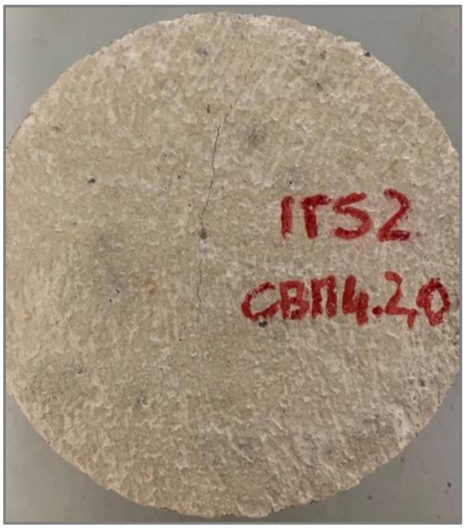

Figure 56-CBM4.2,0, I.T.S. sample, Proctor compaction

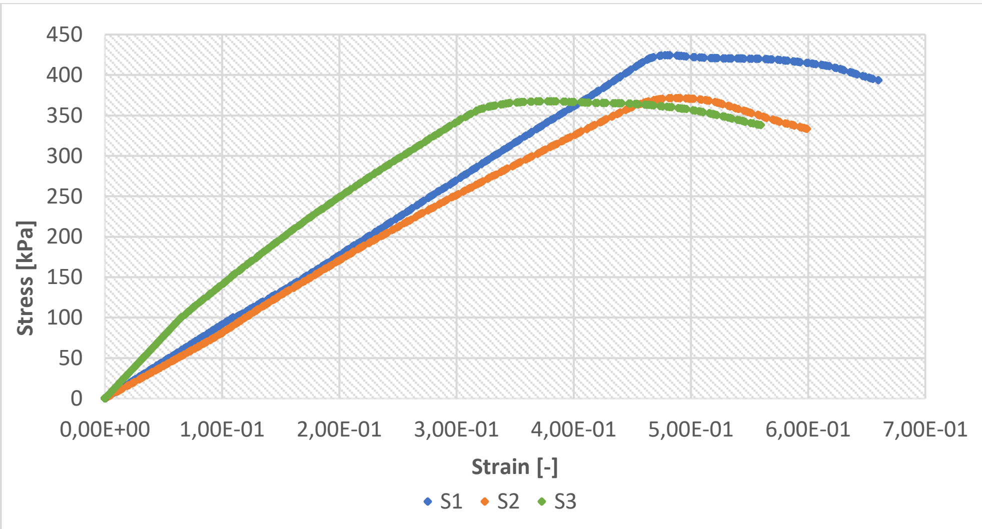

Figure 57-Stress-strain relationship,ITS,CBM4.2,0

Table 41- CBM4.2,0, results of ITS tests

CBM 4.2,0	Max Load (kN)	ITS (MPa)	ITS Average (MPa)	St. dev. (Mpa)
S1	7,50	0,27	0,25	0,02
S2	6,56	0,24		
S3	6,49	0,23		

About the requirements of cement-bound mixtures presented in chapter 1, the minimum acceptable value for ITS is 0,25 MPa. Therefore, according to experimental data, CBM1.2,0 and CBM4.1,5 cannot be accepted.

3.1.5 Gyratory compaction

The effect of compaction methodology on cement-bound mixtures has been investigated by preparing samples in the Gyratory compactor machine. Their sizes were the same as Proctor's samples, particularly 150x120mm. As indicated in sub-chapter 2.1.4, the device can impose a target height or assess a fixed number of gyrations. It has been decided to set 100 gyrations to achieve the target height, even considering a variation of $\pm$ 1cm.

Moreover, the Gyratory compacted samples have been only subjected to indirect tensile tests.

Table 42- CBM samples, Gyratory compaction

CBM	OPTIMUM W (%)	DIMENSION (MM)	N°
CBM1.2,5	6%	150x120	3
CBM4.2,0	6%	150x120	3

3.1.5.1 I.T.S. tests

Figure 58-CBM1.2,5, Gyratory compacted sample

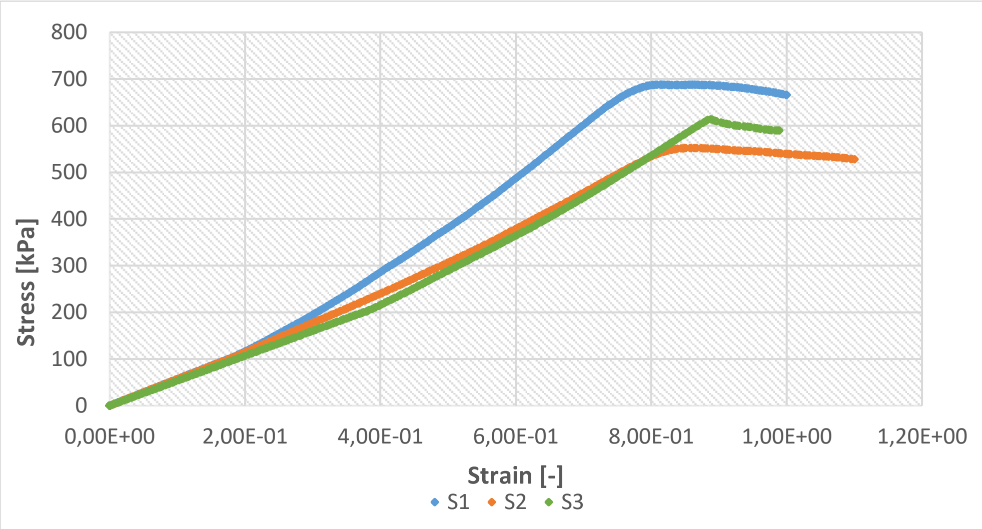

Figure 59-Stress-strain relationship, ITS, Gyratory compaction, CBM1.2,5

Table 43-CBM1.2,5, results of ITS tests, Gyratory compaction

CBM1.2,5	Max Load (kN)	ITS (MPa)	ITS Average (MPa)	St. dev (MPa)
S1	12,16	0,41	0,37	0,04
S2	9,76	0,33		
S3	10,84	0,37		

Figure 60-CBM4.2,0, Gyratory compacted sample

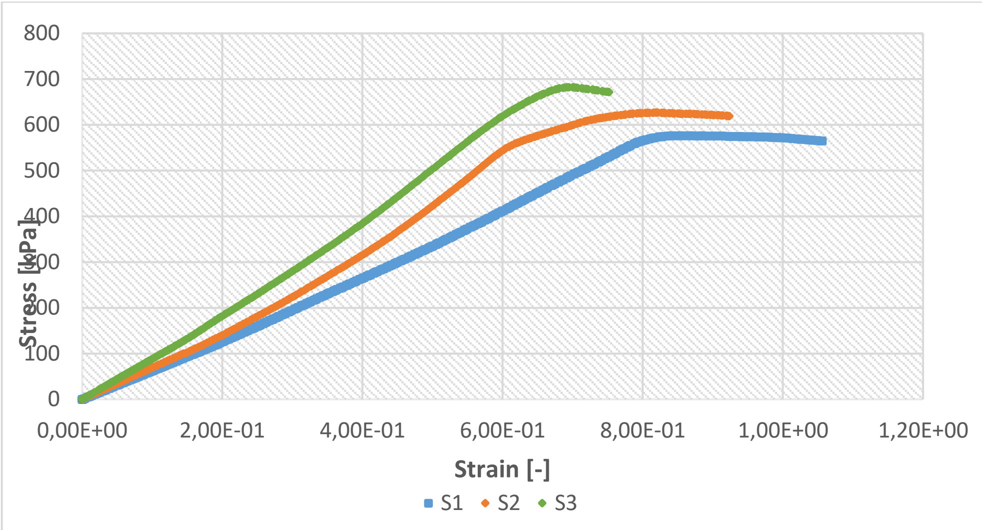

Figure 61-Stress-strain relationship, ITS, Gyratory compaction, CBM4.2,0

Table 44-CBM4.2,0, results of ITS tests, Gyratory compaction

CBM 4.2,0	Max Load (kN)	ITS (MPa)	ITS Average (MPa)	St. dev (MPa)
S1	10,19	0,35	0,38	0,04
S2	11,07	0,38		
S3	12,05	0,42		

3.1.6 Relationship between UCS and ITS

Several studies have been conducted to determine the relationship between the unconfined compressive test and indirect tensile test results. The literature approximates the correlation between UCS and ITS as linear, assuming the ITS as 1/8 and 1/10 of UCS.

Moreover, it has been decided to estimate this relationship from data obtained during this experimental campaign.

Table 45-UCS vs. ITS, experimental results

CBM	UCS (MPa)	ITS (MPa)	ITS/UCS (-)	ITS/UCS average (-)
CBM1.2,0	3,22	0,20	0,06	
CBM1.2,5	3,84	0,29	0,08	0,08
CBM1.3,0	4,99	0,44	0,09	
CBM4.1,5	3,92	0,15	0,04	0,04
CBM4.2,0	5,77	0,25	0,04	

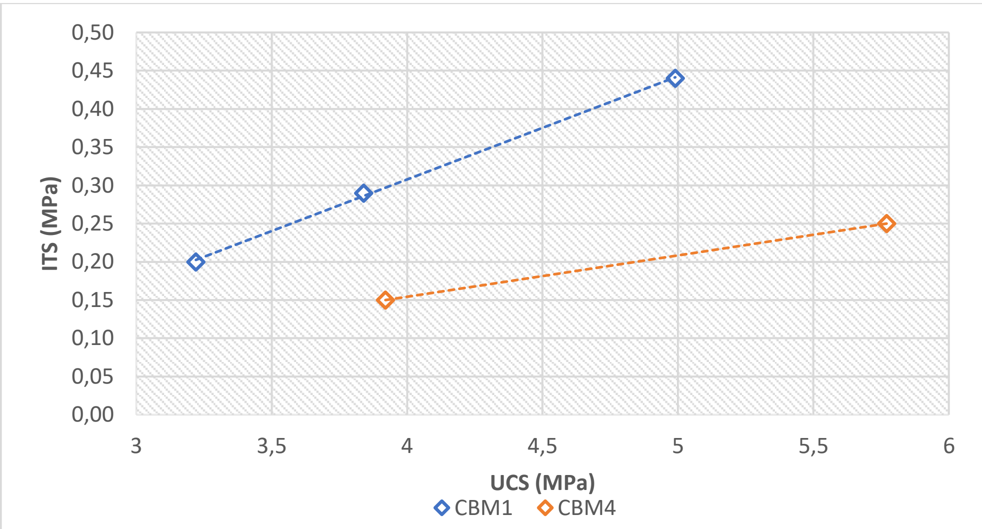

Figure 62-UCS vs. ITS

The linear trend between UCS and ITS has been confirmed from the experimental data. However, differently from the literature, ITS is on average 1/12 of UCS for CBM1 and 1/24 of UCS for CBM4.

ELASTIC MODULI

As specified in Chapter 1, it is possible to estimate the elastic moduli by interpreting test results. Specifically, the stress-strain curvilinear relationships, derived from data analysis of the unconfined compressive tests, give the possibility to derive both tangent and secant modulus and the energy required to fracture the material (toughness).

3.1.7 UCS test

By way of example, in Figures 50 and 51, the same stress-strain curvilinear relationship is reported. Specifically, in Figure 49, the secant and tangent moduli are presented, and in Figure 50, the six-degree polynomial approximating the stress-strain curve is reported. Moreover, the integral of the polynomial, corresponding to the area below the curve, quantify the energy required to fracture the material.

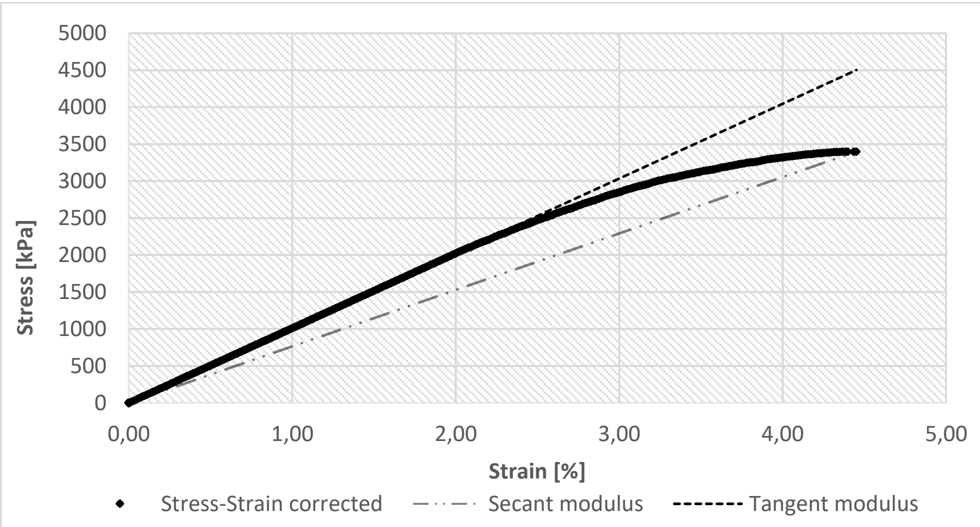

Figure 63-Elastic moduli derived from the stress-strain relationship, CBM1.2,0

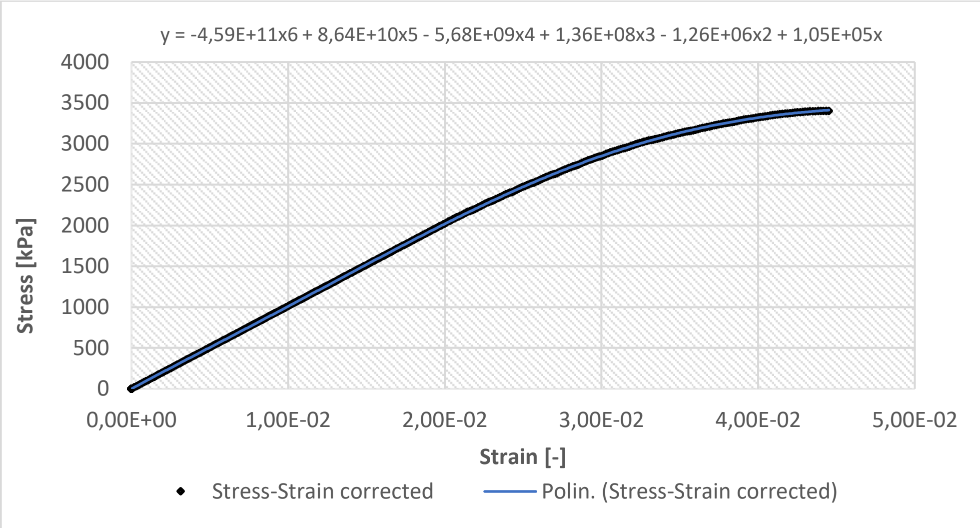

Figure 64-Toughness Elastic derived from the stress-strain relationship, CBM1.2,0

Table 46-Elastic moduli,CBM1

CBM	Secant modulus (MPa)			Tangent modulus (MPa)		
	S1	S2	S3	S1	S2	S3
CBM1.2,0	76,91	76,38	80,17	114,40	101,15	114,74
CBM1.2,5	85,63	-	79,05	101,41	-	110,60
CBM1.3,0	97,33	101,81	91,41	151,33	170,21	120,56

Table 47-Elastic moduli, CBM4

CBM	Secant modulus (MPa)			Tangent modulus (MPa)		
	S1	S2	S3	S1	S2	S3
CBM4.1,5	70,59	75,53	78,33	83,02	89,74	82,49
CBM4.2,0	92,92	88,17	94,49	143,96	120,12	131,98

Table 48-Toughness,CBM1

CBM	Toughness (kPa ·mm/mm)		
	S1	S2	S3
CBM1.2,0	80,53	91,25	73,48
CBM1.2,5	89,78	76,73	105,44
CBM1.3,0	156,38	172,82	161,01

In figure 43, the missing values refer to the outliers of the UCS tests; therefore, these results were deleted.

Table 49-Toughness, CBM4

CBM	Toughness (kPa ·mm/mm)		
	S1	S2	S3
CBM4.1,5	136,62	118,64	179,02
CBM4.2,0	224,57	223,93	211,50

Table 50-Resume of stress-strain relationship data

CBM	Secant modulus (MPa)	Tangent modulus (MPa)	Toughness (kpa ·mm/mm)
CBM1.2,0	77,82	110,10	81,75
CBM1.2,5	82,34	106,00	97,61
CBM1.3,0	96,85	147,37	163,40
CBM4.1,5	74,82	85,08	144,76
CBM4.2,0	91,86	132,02	220,00

4 DATA ANALYSIS

This chapter is dedicated to data analysis. All results obtained during the experimental campaign are here analysed to meet the objectives of the research work.

INFLUENCE OF CEMENT CONTENT

One of the objectives of this research work was the definition of the influence of cement content on cement-treated base material properties. Although the most interesting influence of cement is on mechanical properties, the effect on physical properties and elastic parameters has been included.

4.1.1 Influence of cement content on mechanical properties

The influence of cement dosage on mechanical properties has been investigated by subjecting Proctor samples of CBM1 and CBM4 to mechanical tests, as described in sub-chapters 3.1.4.1.1 and 3.1.4.1.2.

Table 51- Resume of UCS tests results, CBM1

CBM	Max Load (kN)	UCS (MPa)	Dev st. (MPa)
CBM 1.2,0	56,85	3,22	0,16
CBM 1.2,5	67,79	3,84	0,17
CBM 1.3,0	88,19	4,99	0,17

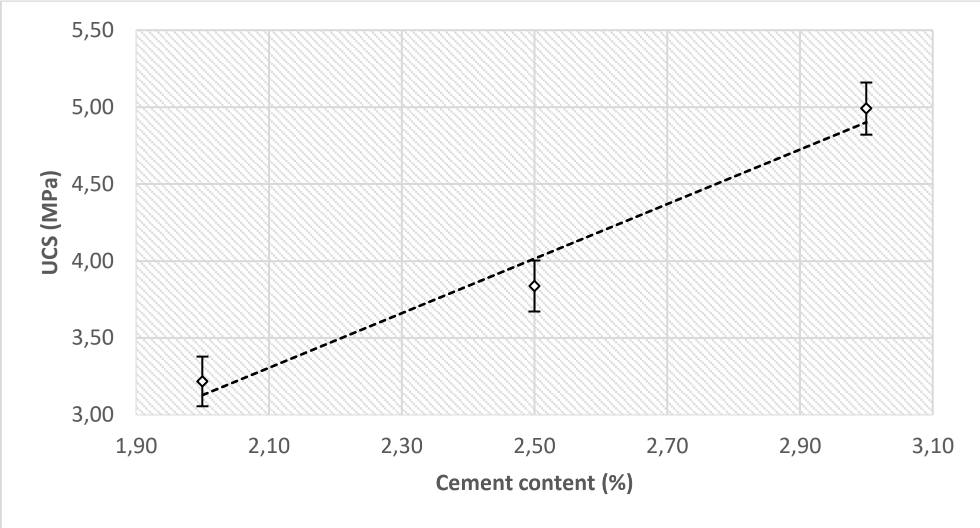

Figure 65- UCS vs. cement content, CBM1

Table 52-Resume of UCS tests results, CBM4

CBM	Max Load (kN)	UCS (MPa)	St. dev (Mpa)
CBM 4.1,5	69,31	3,92	0,22
CBM 4.2,0	101,99	5,77	0,04

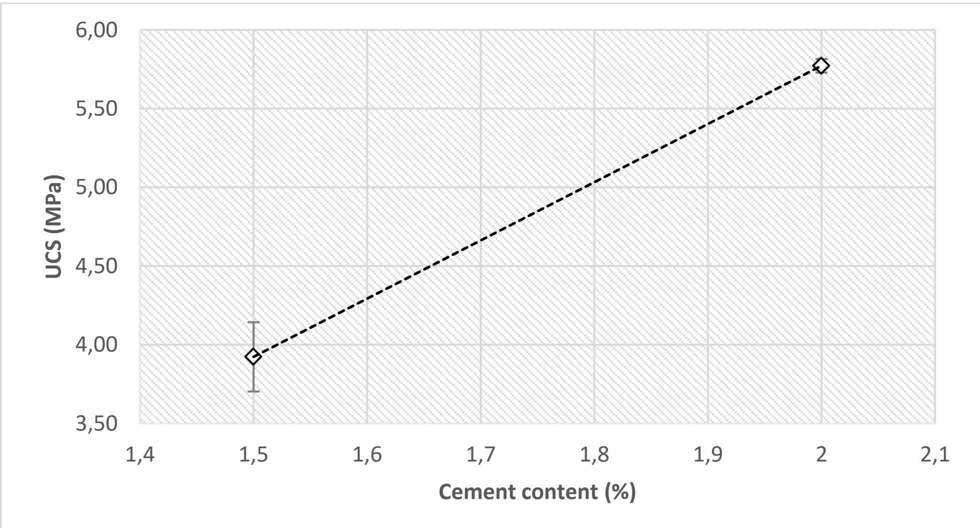

Figure 66-UCS vs. cement content, CBM4

Based on experimental data obtained, the increase in cement contents for CBM1 and CBM4 results in a growth in UCS value. Moreover, in Figure 56, the cement content is related to the UCS, and the trendline highlight a linear relationship between the quantities. However, differently from the linear behaviour clearly defined for CBM1, for CBM4 specific trends cannot be observed for lack of experimental data. However, the expectation is that, also in this case, the trend is linear.

Table 53-Resume of ITS tests results, CBM1

CBM	Max Load (kN)	ITS (MPa)	St. dev (MPa)
CBM 1.2,0	5,57	0,20	0,01
CBM 1.2,5	8,20	0,29	0,04
CBM 1.3,0	12,52	0,44	0,05

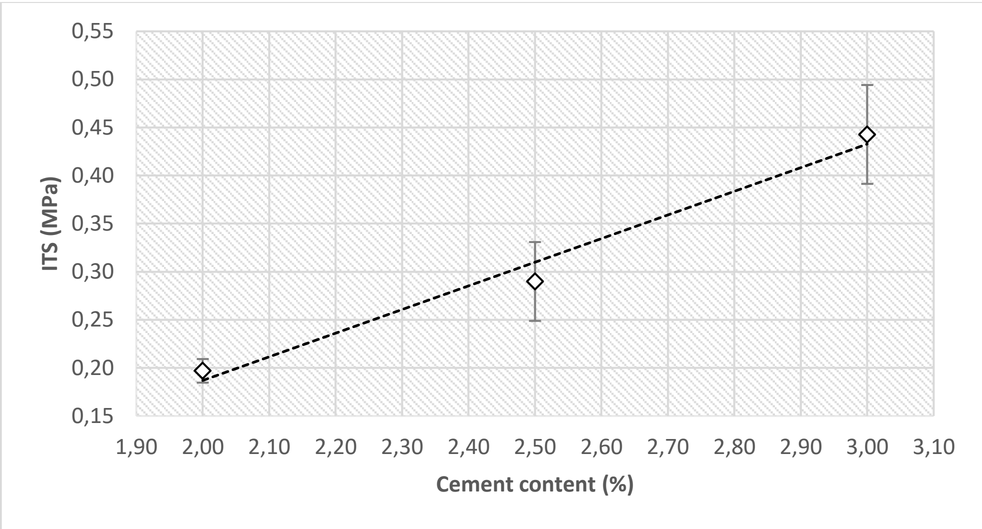

Figure 67-ITS vs. cement content, CBM1

Table 54-Resume of ITS tests results, CBM4

CBM	Max Load (kN)	ITS (MPa)	St. dev (Mpa)
CBM 4.1,5	4,12	0,15	0,01
CBM 4.2,0	6,85	0,25	0,02

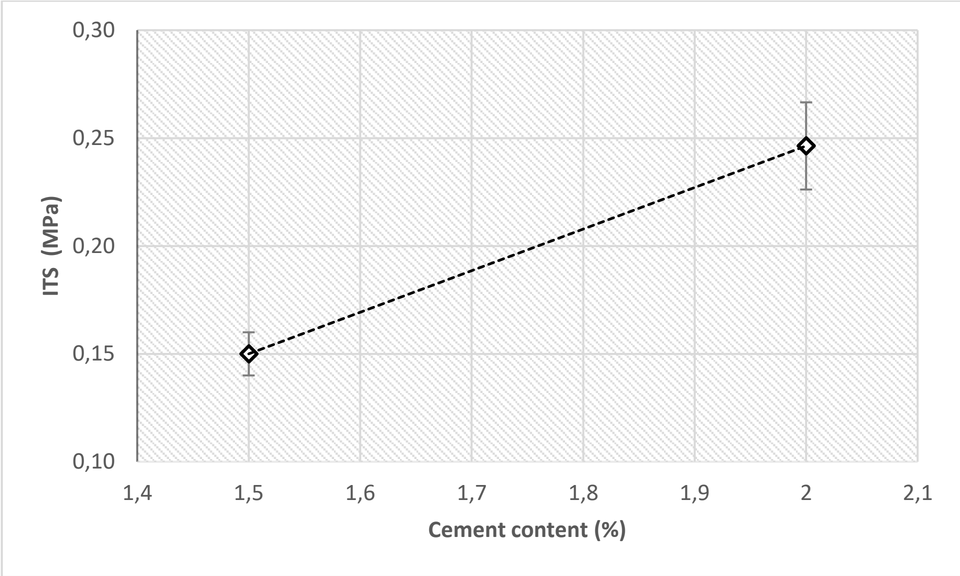

Figure 68-ITS vs. cement content, CBM4

The first consideration is about the more excellent repeatability of ITS results than the UCS ones, indicated by very low standard deviations. Moreover, as was expected, the augment of cement dosage results in a linear increase of ITS value.

4.1.2 Influence of cement content on dry density

In investigating the influence of cement dosage on dry densities, the two cement-bound mixtures proctor bells have been compared to the ones of the respective granular mixtures.

4.1.2.1 GM1 vs. CBM1

As explained in the experimental results, the cement-bound mixture CBM1 has been designed by adding different cement contents to GM1. By comparing Proctor tests' results performed on CBM1 mixtures with GM1, it has been possible to indagate the influence of cement on dry density.

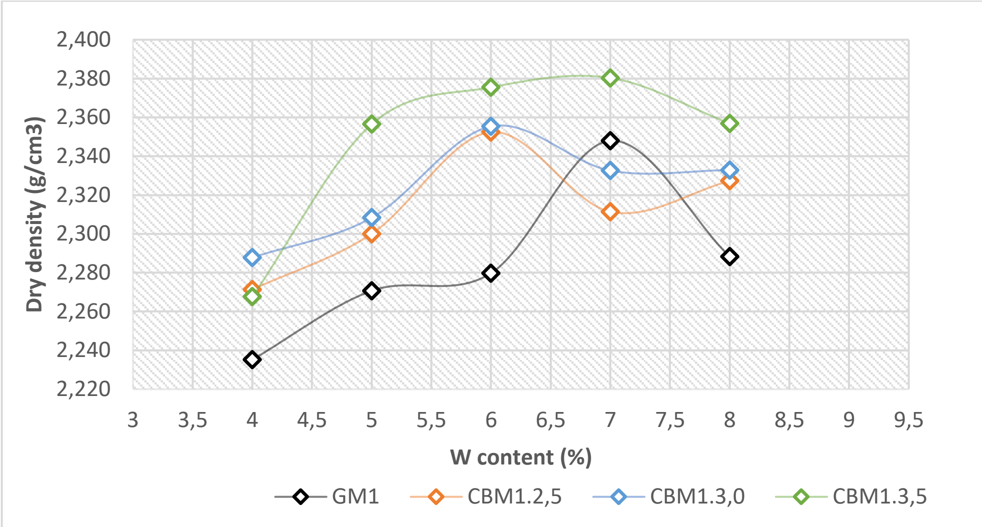

Figure 69-Effect of cement on dry density, GM1 vs. CBM1

Table 55-Dry densities results, GM1 vs. CBM1

W CONTENT (%)	DRY DENSITY (G/CM3)			
	GM1	CBM1.2,5	CBM1.3,0	CBM1.3,5
4	2,235	2,271	2,288	2,268
5	2,271	2,300	2,308	2,356
6	2,280	2,352	2,356	2,375
7	2,348	2,311	2,333	2,380
8	2,288	2,327	2,333	2,357

Referring to experimental results in Figure 49 and Table 52, the increment of cement dosage significantly increases the dry density. Moreover, dry densities at the optimum water contents have been compared to indagate the growth trend.

Table 56- Dry densities comparison, GM1 vs. CBM1

Mixtures	Optimum w content (%)	Dry density (g/cm3)
GM1	7	2,348
CBM1.2,5	6	2,352
CBM1.3,0	6	2,356
CBM1.3,5	7	2,380

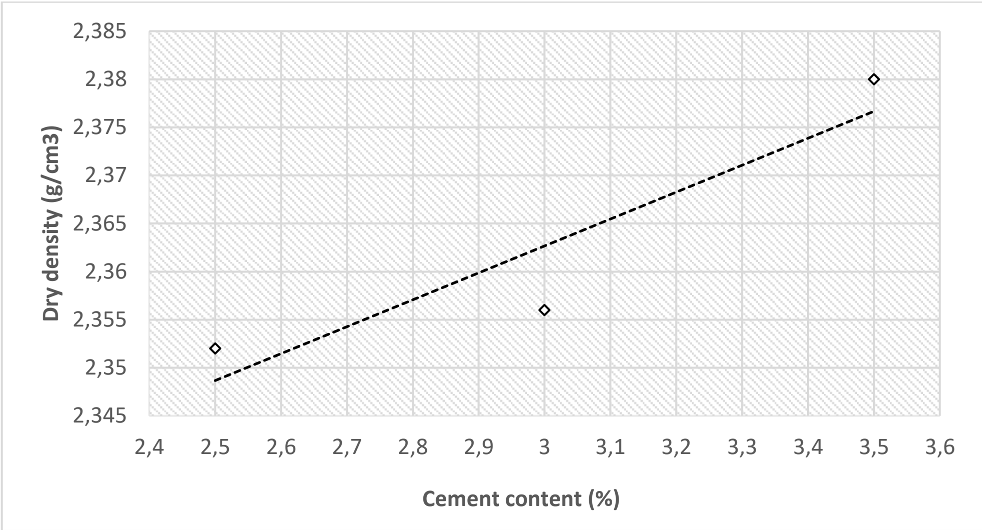

Figure 70-Cement content vs. Dry density, CBM1

As represented in Figure 53, the growth trend between cement content and dry density is linear. In conclusion, this behaviour is due to the lack of fine fractions in the mixtures. Therefore, as the finer fraction, the cement saturates the voids and consequently increases the dry density.

4.1.2.2 GM4 vs. CBM4

As introduced in the experimental results, CBM4 has been designed by varying cement contents to GM4. Proctor tests' results of CBM4 and GM4 mixtures are therefore compared to analyse the influence of cement on dry density.

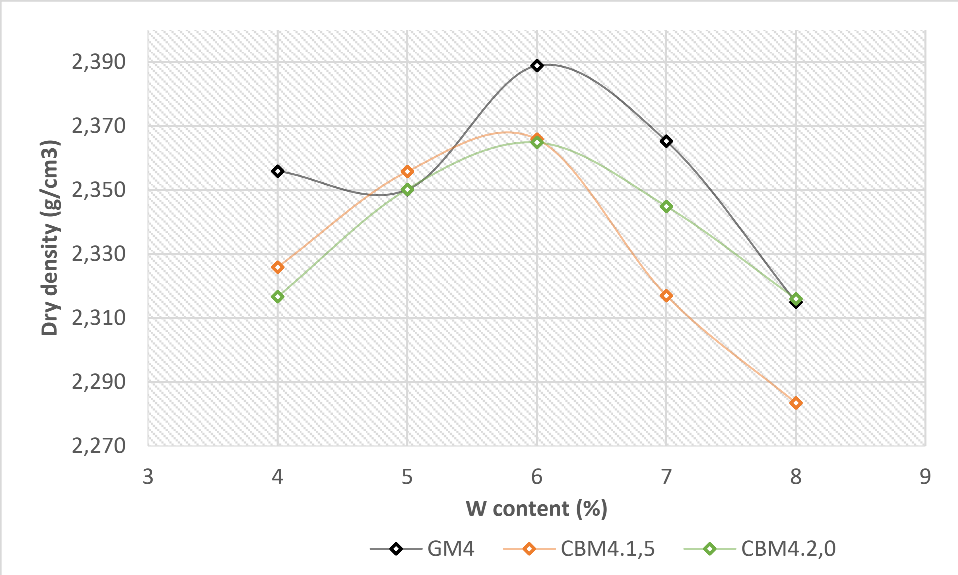

Figure 71-Effect of cement on dry density, GM4 vs. CBM4

Table 57-Dry densities results, GM4 vs. CBM4

CONTENT (%)	**DRY DENSITY (G/CM3)**		
	GM4	CBM4.1,5	CBM4.2,0
4	2,356	2,326	2,317
5	2,350	2,356	2,350
6	2,389	2,366	2,365
7	2,365	2,317	2,345
8	2,315	2,283	2,316

According to the experimental results, differently from what was obtained for CBM1, the addition of cement results in dry densities decrement. Moreover, it is crucial to remark the higher percentage of fine fraction due to the addition of mineral filler in these mixtures since it is the reason for this behaviour. If for CMB1, the cement as the finer fraction filled the voids, increasing dry densities, for CBM4, the voids were already filled by mineral filler.

4.1.3 Influence of cement content on elastic parameters

The results obtained from the stress-strain relationships, obtained by U.C.S and I.T.S tests, have been compared to the cement content. Specifically, the influence of cement content on elastic parameters, such as the elastic moduli and the toughness, have been investigated.

Table 58-Resume of elastic parameters, CBM1

CBM	Secant modulus (MPa)	Tangent modulus (MPa)	Toughness (kPa ·mm/mm)
CBM 1.2,0	77,82	110,10	81,75
CBM 1.2,5	82,34	106,00	97,61
CBM 1.3,0	96,85	147,37	163,40

Table 59- Standands deviations on elastic parameters, CBM1

Mixture	Secant Modulus	Tangent Modulus
	St. dev (MPa)	St. dev (MPa)
CBM1.2,0	2,05	7,75
CBM1.2,5	4,66	6,50
CBM1.3,0	5,22	25,06

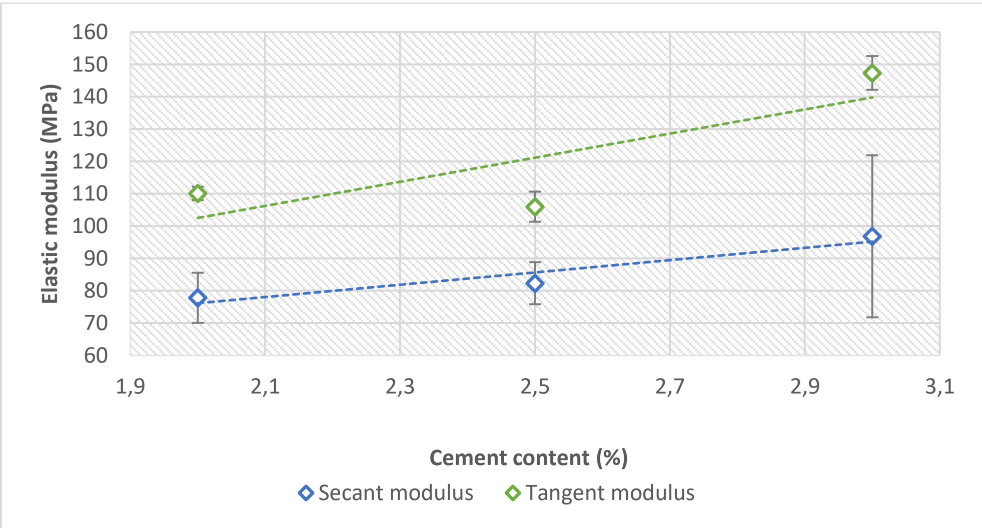

Figure 72-Elastic moduli vs. cement content, CBM1

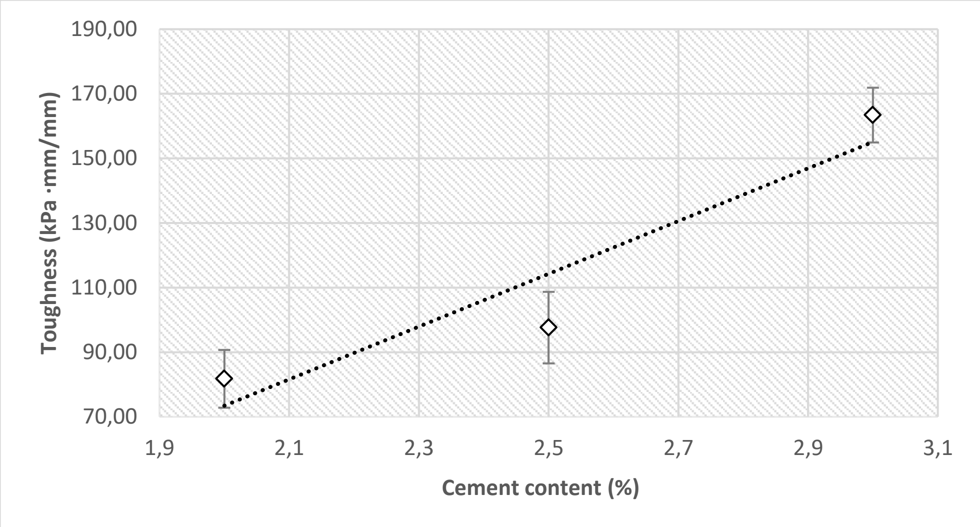

Figure 73-Toughness vs. cement content, CBM1

Table 60-Resume of elastic parameters, CBM4

CBM	Secant modulus (MPa)	Tangent modulus (MPa)	Toughness (kPa ·mm/mm)
CBM 4.1,5	74,82	85,08	144,76
CBM 4.2,0	91,86	132,02	220,00

Table 61-Standand deviations on elastic parameters,CBM4

CBM	Secant Modulus St. dev (MPa)	Tangent Modulus St. dev (MPa)	Toughness St. dev (MPa)
CBM4.1,5	3,92	4,04	31,00
CBM4.2,0	3,29	11,92	7,37

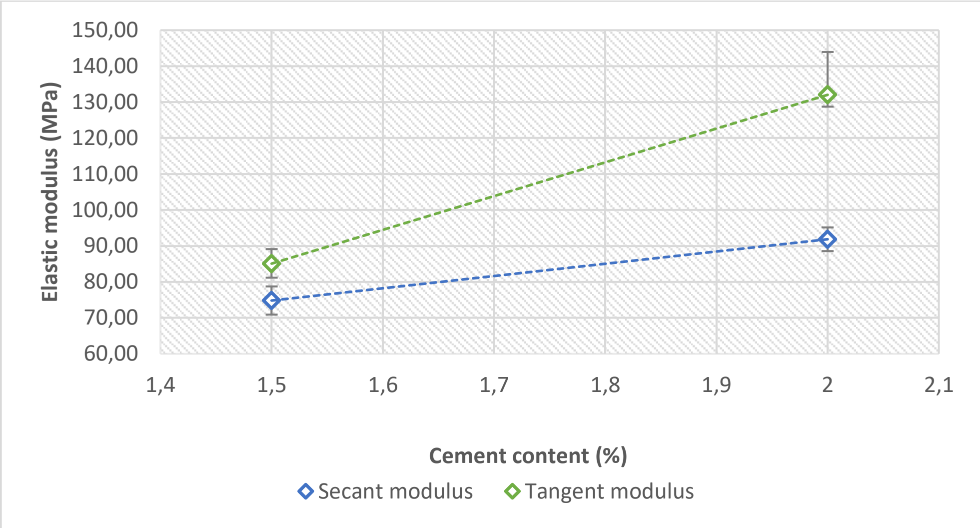

Figure 74-Elastic moduli vs. cement content, CBM4

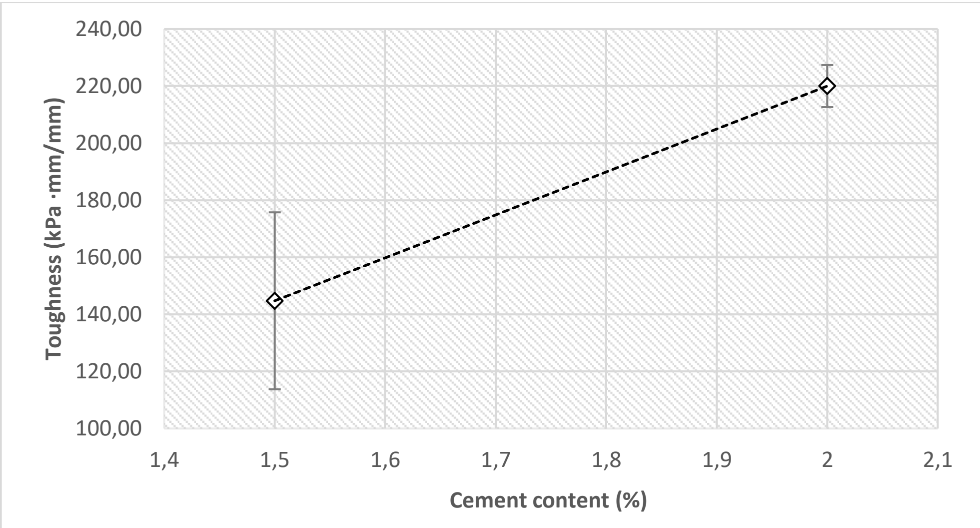

Figure 75-Toughness vs. cement content, CBM4

The experimental results highlighted a linear increase in the elastic moduli and toughness due to the rise of cement content. This behaviour was expected since the elastic parameters are strictly linked to mechanical properties, particularly the unconfined compressive strength, which increases linearly with the cement content.

INFLUENCE OF WATER CONTENT ON I.T.S.

The influence of water content on mechanical properties has been investigated on ITS since it is the most repeatable test. The bound-mixture selected for the tests was CBM4.2,0. Specifically, for each water content of the Proctor bell, only one cylindrical sample, 150x120mm, has been tested due to the high repeatability of the ITS test.

Table 62-Effect of water content on ITS, CBM4.2,0

W content (%)	Max Load (kN)	ITS (MPa)
4	13,24	0,47
5	12,34	0,44
6	6,85	0,25
7	5,21	0,18
8	2,51	0,09

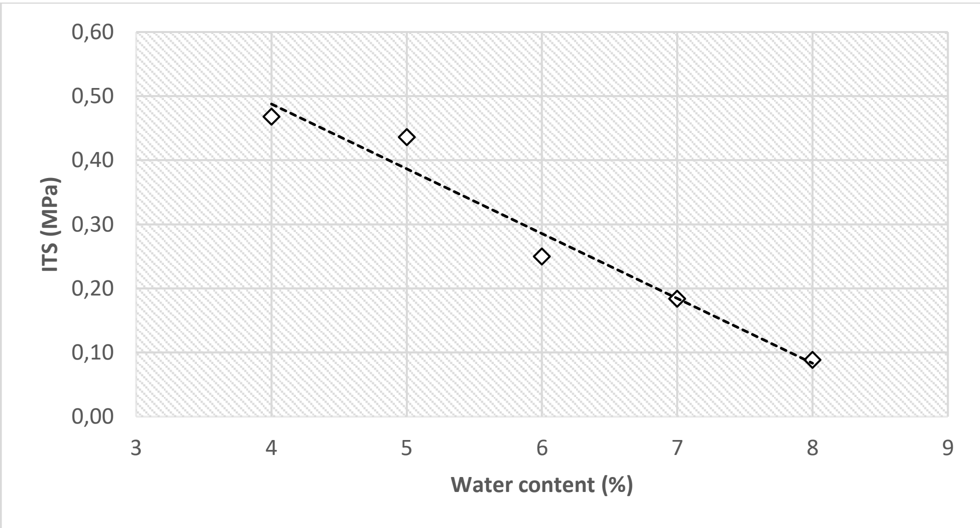

Figure 76-Water content vs. ITS, CBM4.2,0

As the experimental results suggest, the increase of water content translates into ITS linear degrowth.

INFLUENCE OF MINERAL FILLER ON DRY DENSITY

Another objective of the research work was defining the effect of mineral filler on dry densities. Two granular mixtures were designed during the experimental campaign considering a percentage of mineral filler, $CaCO_3$ in GM3 and FLOWFILL in GM4.

The effect of the two fillers on dry densities has been investigated by comparing the results obtained by Modified Proctor tests since the two granular mixtures have the same lithic skeleton of GM2.

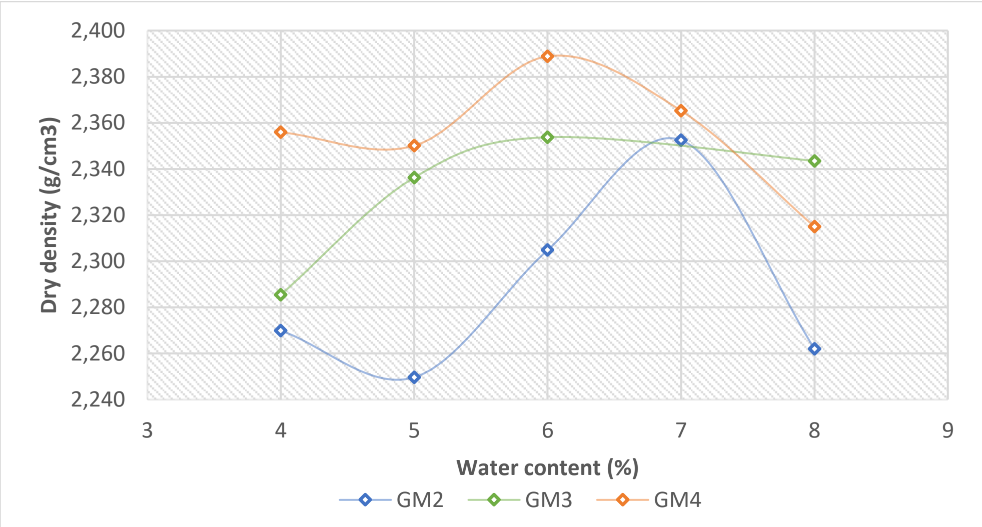

Figure 77-Mineral filler vs. dry density

Table 63-Comparison between GMs

Water content (%)	GM2	GM3	GM4
4	2,270	2,285	2,356
5	2,250	2,336	2,350
6	2,305	2,354	2,389
7	2,352	-	2,365
8	2,262	2,343	2,315

The experimental results show an increase in dry densities due to the addition of mineral filler. The lack of fines in GM2 can justify this behaviour. All the previous voids present in the mixtures are now filled by mineral filler since it is the finer aggregate class, increasing dry density.

INFLUENCE OF COMPACTION METHODOLOGY

Figure 78-Proctor sample vs. Gyratory sample

Differently from what was prescribed, in the last part of the experimental plan, it has been decided to compact samples with the Gyratory compaction apparatus.

The objective was to define the effect of compaction methodology on mechanical and physical properties. I.T.S. has been chosen as the yardstick for mechanical properties since it is the more repeatable test, whereas dry density has been selected for the physical properties.

Six samples have been prepared, setting 100 gyrations to achieve the target height of 120mm: three of CBM1.2,5 and three of CBM4.2,0. Unlike Proctor's samples, which sizes were precise 150x120, the obtained Gyratory samples were a little taller. Moreover, as shown in Figure 67, the Gyratory compaction results in an inhomogeneous aggregate distribution and holes were present on the specimen surface. The two compaction methodologies are highly different; indeed, Gyratory compaction is achieved by the concomitant action of low static compression and shearing action, while Proctor compaction is performed by layers and by the blows of a falling rammer.

4.1.4 Influence of compaction methodology on dry density

The effect of compaction methodology on dry density has been investigated by analysing the results of Gyratory compaction tests. Specifically, the machine gives the height of samples related to the number of gyrations performed; therefore, it has been possible to derive the volumes and then the densities.

Figure 79-Number of gyrations vs. dry density, CBM1.2,5

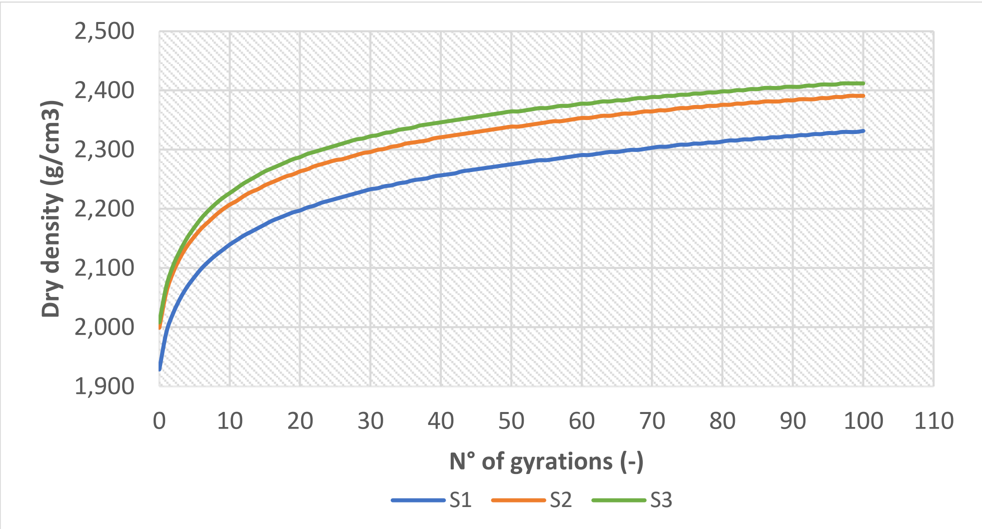

Figure 80-Number of gyrations vs. dry density, CBM4.2,0

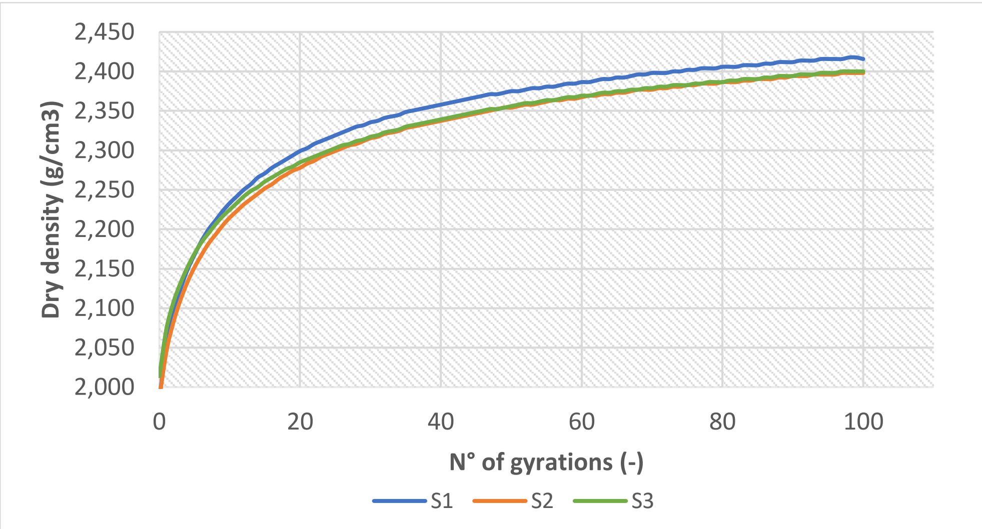

Table 64-Proctor vs. Gyratory, comparison between densities

	Dry density (g/cm3)	
CBM	Proctor	Gyratory
CBM1.2,5	2,353	2,378
CBM4.2,0	2,365	2,405

According to the experimental results collected in Table 64, the Gyratory compaction achieved higher densities than the Proctor one. The explanation of this result derives from the two different methodologies of compaction. Proctor compaction is performed by layers, and the mechanical action of the hammer causes the larger aggregates to be split, allowing closer arrangements of granules. Instead, in the Gyratory apparatus, the static compression and the shearing action resulting from the motion of the samples' axis led just to a granules redistribution and reorganization but not to an optimal meshing. However, even if the samples produced by Gyratory compaction were irregular higher densities have been achieved.

4.1.5 Influence of compaction methodology on I.T.S.

Compaction methodology's influence on mechanical properties has been investigated. Samples have been subjected to indirect tensile tests since they are the most repeatable ones. Therefore, the results, presented in chapter 4.1.6.1, are compared in Tables 65 and 66 with Proctor's samples results.

Table 65-Compaction methodology vs. ITS, CBM1.2,5

	Samples	Dimensions (mm)	ITS (MPa)
CBM1.2,5	Proctor compaction	150x120	0,29
CBM1.2,5	Gyratory compaction	150x126	0,37

Table 66-Compaction methodology vs. ITS, CBM4.2,0

	Samples	Dimensions (mm)	ITS (MPa)
CBM4.2,0	Proctor compaction	150x120	0,25
CBM4.2,0	Gyratory compaction	150x123	0,38

As expected from the higher densities achieved, the experimental results indicate an increase in ITS value due to the Gyratory compaction method.

5 CONCLUSIONS

The primary purpose of this research was to evaluate the variation of physical and mechanical properties of cement-treated base materials at modifying some parameters.

The main finding relates to the effect of cement content. Therefore, the experimental results demonstrated its linear relationship with mechanical properties, particularly the unconfined compressive strength and the indirect tensile strength. Relatively to this, an observation about the cement effect on dry density has been included, and a linear growing trend has been obtained. The role of cement relates to the lack of fine fraction in the mixture; indeed, it saturates the voids and consequently causes an increase in dry density. The effect of cement content has also been investigated on elastic parameters such as the elastic moduli and the toughness. Since they are strictly related to mechanical properties, the obtained result was also a linear relationship between quantities.

Nevertheless, the influence of water content has also been indagated regarding mechanical properties. The indirect tensile tests results underlined linear degrowth of ITS value related to the rise of water content.

The effect of the mineral filler on dry densities has been considered about physical properties. Similar to cement's behavior, the mineral filler, being the finer fraction, saturates the voids leading to higher dry densities.

In conclusion, the additional samples produced by Gyratory compaction have brought exciting results. The visual impact of the compaction was not wholly acceptable since the visible inhomogenous aggregate distribution and the presence of holes on the surface of the specimens. However, the compaction led to higher densities than Proctor's compaction, and the indirect tensile strengths were even greater. The difference in dry densities is due to the different compaction modes: Proctor compaction is performed by layers, and the mechanical action of the hammer causes the larger aggregates to be split, allowing closer arrangements of granules; instead, the Gyratory compaction leads to granules redistribution and reorganization but not to an optimal meshing. The Gyratory compaction apparatus is not usually used for cement-bound mixtures, but according to the surprising results obtained, it would be worth dwelling on the question.

Finally, enough cement should be added to mixtures to meet the desired engineering properties. Moreover, specific requirements have been introduced regarding cement-bound mixtures, and all the designed mixtures have been adequately checked for acceptability. For what concerned CBM1, only the mixture containing the 2,0% of cement results in poor mechanical properties, whereas, for CBM4, the mixture containing the 1,5% did not exceed the minimum threshold in tension. Reminding that more cement than required is not economical and leads to cracking, the two cement-bound mixtures comparable were CBM1.2,5 and CBM4.2,0 since they are the first over the acceptability thresholds. According to this, it is clear that the improvement of particle size distribution in CBM4 by adding mineral filler would result in a reduction of 0,5% of cement content for meeting the criteria. This finding could lower production costs, reduce the percentage of cement in the mixture, and limit damages since lower cement contents would prevent the formation of wider reflective cracks.

6 BIBLIOGRAPHY

[1] Mena I. Souliman , Nitish R. Bastola , Waleed A. Zeiada. *Mechanistic and Cost-Effectiveness Analysis of Cement Treated Bases in Flexible Pavement*, (2020) The University of Texas at Tyler

[2] Cruzado D.A.. *Design of long life pavements based on thin high strength cement bound bases M7/M8 Portlaoise motorway experience (Ireland)*, (2011) Head of Ground Engineering Consultancy. Eptisa

[3] European Asphalt Pavement Association [EAPA]. *Long-Life Asphalt Pavements*, (2007) Technical version

[4] Ferne B.. *Long-life pavements—a European study by ELLPAG*,(2006) International Journal of Pavement Engineering, 7:2, 91-100, DOI: 10.1080/10298430600619059

[5] Hernando D. , Miguel A. del Val.. *Guidelines for the design of semi-rigid long-life pavements*, (2016) International Journal of Pavement Research and Technology

[6] Kolhe P.S.. *Experimental Study on Use of Cemented Materials for Pavements,*(2007) M.Tech, Civil Engineering Department, I.I.T. Kanpur-208

[7] Iowa State University. *Guide to cement-based integrated pavements solutions,* (2011) Institute for Transportation

[8] Hassan, El-Hussain, Al-Kuwari, Al-Emadi. *Development and Performance of Cement Bound Materials in Road Pavements*, (2020) International Conference on Civil Infrastructure and Construction (C.I.C. 2020)

[9]Portland cement association [P.C.A.]. *Cement-Treated Base (C.T.B.),(2019)*

[10] Portland cement association [P.C.A.]. *Cement-Treated Base,(2019) Integrated paving solutions*

[11]Halsted G.E., Luhr D.R., Adaska W. S.. *Guide to Cement-Treated Base (C.T.B.),(2006) Portland cement association [P.C.A.]*

[12]Garber S., Rasmussen R.O , Harrington D.. *Guide to Cement-Based Integrated Pavement Solutions*,(2011) Portland Cement Association, 61-64

[13] European standard EN14227-1, *Hydraulically bound mixtures - Specifications - Part 1: Cement bound granular mixtures* (2013)

[14]Portland cement association [P.C.A.]. *Soil-cement for Commercial Sites.* The low-cost alternative for heavy-duty industrial pavements

[15] Adaska W. S., Luhr D. R.. *Control of reflective cracking in cement stabilized pavements,* (2004) Cracking in Pavements – Mitigation, Risk Assessment and Prevention

[16] Haifang W. et al.. *Characterization of Cementitiously Stabilized Layers for Use in Pavement Design and Analysis,* (2014) National Cooperative Highway Research Program, NCHRP Report 789

[17] Halsted G.E., P.E.. *Minimizing Reflective Cracking in Cement-Stabilized Pavement Bases,(2010) Portland cement association [P.C.A.],* Paper prepared for presentation at the Pavement Maintenance and Preservation Session of the 2010 Annual Conference of the Transportation Association of Canada Halifax, Nova Scotia

[18] Scullion. T., P.E. *Field Investigation: Pre-Cracking of Soil-Cement Bases to Reduce Reflection Cracking,(2001)* Paper Submitted for Presentation and Publication In the 2002 Annual Meeting of Transportation Research Board Washington, D.C.

[19] Portland cement association [P.C.A.], *Reflective Cracking in Cement Stabilized Pavements,(2003)*

[21] Ministero delle infrastrutture e dei trasporti. *Capitolato speciale d'appalto tipo per lavori stradali*, (2019) Formazione di strati in misto cementato, Art. 4

[23] Garcia-Hernández A. et al.. *Self-healing of reflective cracks in asphalt mixtures by the action of encapsulated agents,* (2020) Construction and Building Materials 252

[24] Evirgen B. et al.. *Experimental Performance of Polyester-Fiber-Based Soil Geogrids against Reflective Cracks,(2021)* Transportation Research Record: Journal of the Transportation Research Board

[26] Chakravarthi S., Shankar S. *Utilization of recycled aggregates in cement-treated bases: a state-of-the-art review,* (2021) Innovative Infrastructure Solutions (2021) 6:191

[27] Murray R. et al.. *Demonstrating the Worth of Recycled Aggregates—A Case Study from Qatar,*(2016) Geo-Chicago 2016 GSP 270

[28] Cooley A.. *Effects of Reclaimed Asphalt Pavement on Mechanical Properties of Base Material,*(2015) Theses and Dissertations. 696.

[29] Brown A.V.. *Cement Stabilization of Aggregate Base Materials Blended with Reclaimed Asphalt Pavement (2007)* Brigham Young University, Theses and Dissertation. 428

[30] Yuan D.. *Evaluation and Mix Design of Cement-Treated Base Materials with High Content of Reclaimed Asphalt Pavement* (2011)

[31] Liu J., Yu B., Wang Q.. *Application of steel slag in cement-treated aggregate base course,* (2020) Journal of Cleaner Production, Volume 269

[32] Kasu S.R., Manupati K., Muppireddy R.A. *Investigations on design and durability characteristics of cement-treated reclaimed asphalt for base and subbase layers* (2020) Construction and building material. Volume 252.

[33] Pasetto M., Baldo N.. *Recycling of waste aggregate in cement bound mixtures for road pavement bases and sub-bases (2016)* Construction and building material 108, 112-118

[34] Krawczy B. and Sydlo A.. *Assessment criteria of the recycled aggregate cement bound bases,* (2019) Roads and bridges, 109-126

[35] Sounthararajah A. et al.. *Effect of Cement on the Engineering Properties of Pavement Materials,* (2016) Materials Science Forum. Volume 866, 31-36

[36]Songtao L.. *Strength and fatigue performance for cement-treated aggregate base materials,* (2021) International Journal of Pavement Engineering. Volume 22

[37] Nusit K. et al.. *Advanced Characteristics of Cement-Treated Materials with respect to Strength Performance and Damage Evolution, (2016)* Journal of Materials in Civil Engineering

[38] Zollinger D. G.. *Estimation of the Compressive Strength and Modulus of Elasticity of Cement-Treated Aggregate Base Materials* (2003) Transportation research record journal of the transportation research board.

[39] Thomson M.R.. *Mechanistic Design Concept for Stabilized Base Pavements,* (1986) Civil Engineering Studies, Transportation Engineering Series No.46, University of Illinois, Urbana, IL

[40] Panaro M., *PROGETTO DI PAVIMENTAZIONI SEMIRIGIDE CON FONDAZIONE IN MISTO CEMENTATO. INDAGINI SPERIMENTALI E ANALISI STRUTTURALI*, (2018) Politecnico di Torino, Tesi di Laurea Magistrale

[41] Draft TRH13, *CEMENTITIOUS STABILIZERS IN ROAD CONSTRUCTION*, (1986) TECHNICAL RECOMMENDATIONS FOR HIGHWAYS, 9-10

[42] Austroads, *Cemented Materials Characterisation: Final Report*, (2014) Project No. TT1664

7 ANNEX 1

ELASTIC MODULI DERIVED FROM STRESS-STRAIN RELATIONSHIPS

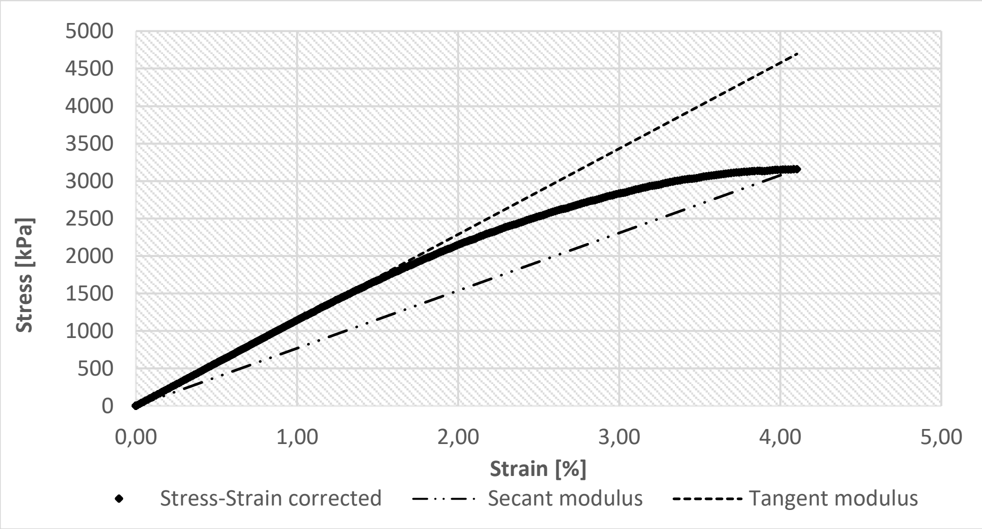

Figure 81- Elastic moduli derived from the stress-strain relationship ,CBM1.2,0 S1

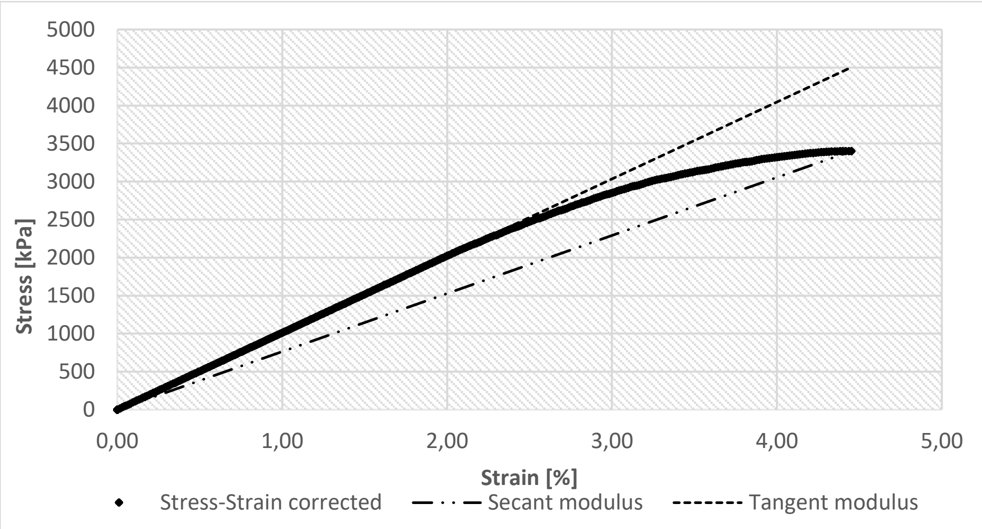

Figure 82- Elastic moduli derived from the stress-strain relationship ,CBM1.2,0 S2

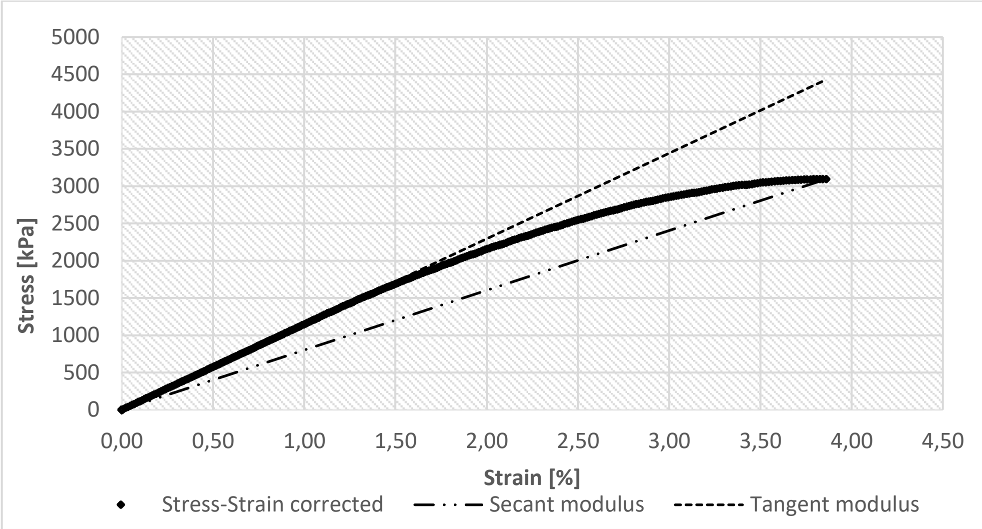

Figure 83- Elastic moduli derived from the stress-strain relationship ,CBM1.2,0 S3

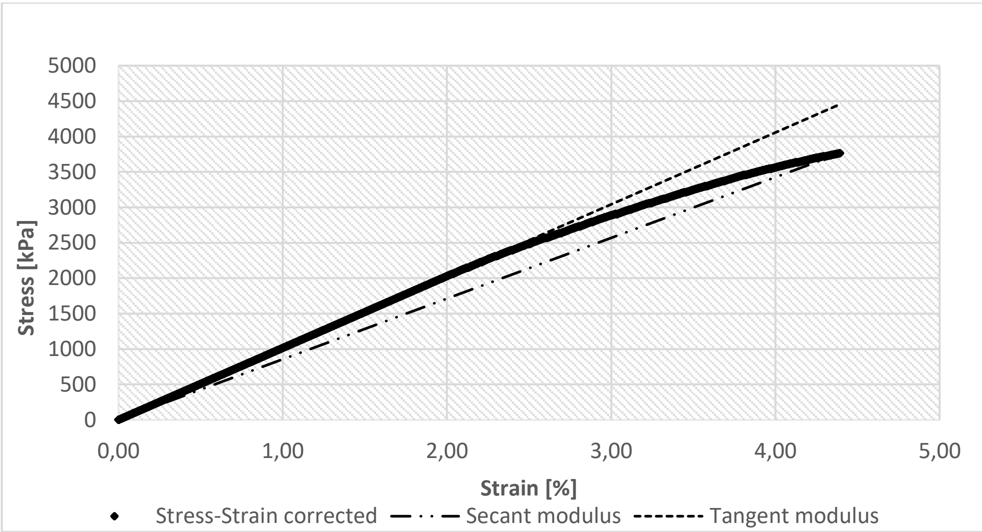

Figure 84- Elastic moduli derived from the stress-strain relationship ,CBM1.2,5 S1

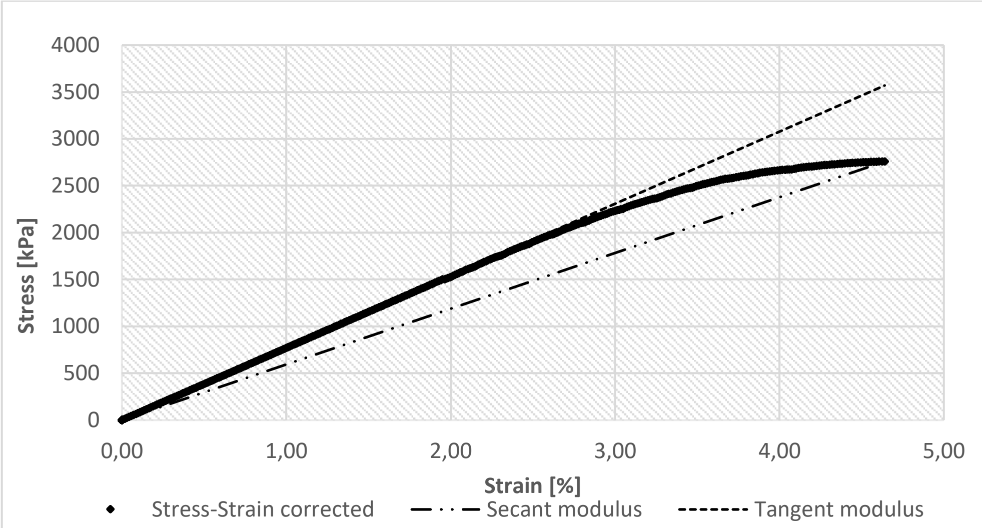

Figure 85- Elastic moduli derived from the stress-strain relationship ,CBM1.2,5 S2

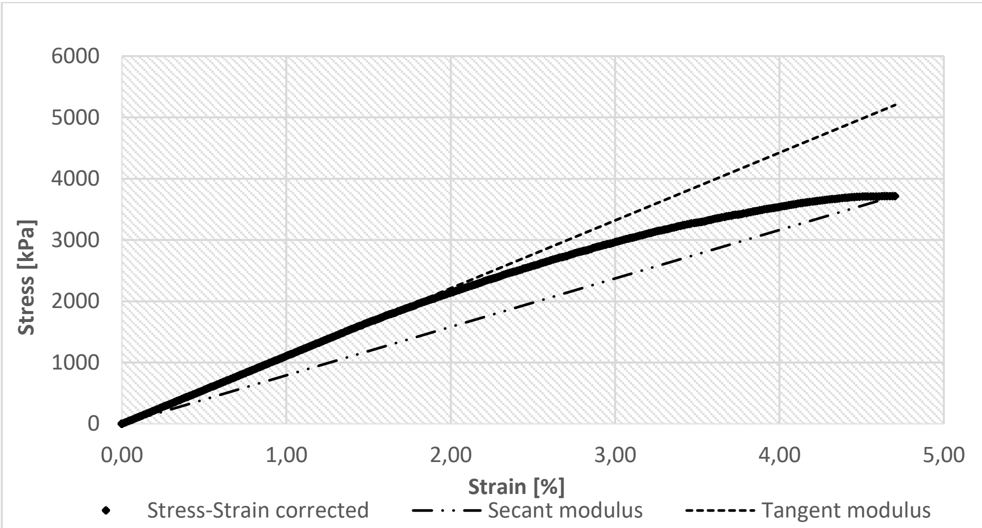

Figure 86- Elastic moduli derived from the stress-strain relationship ,CBM1.2,5 S3

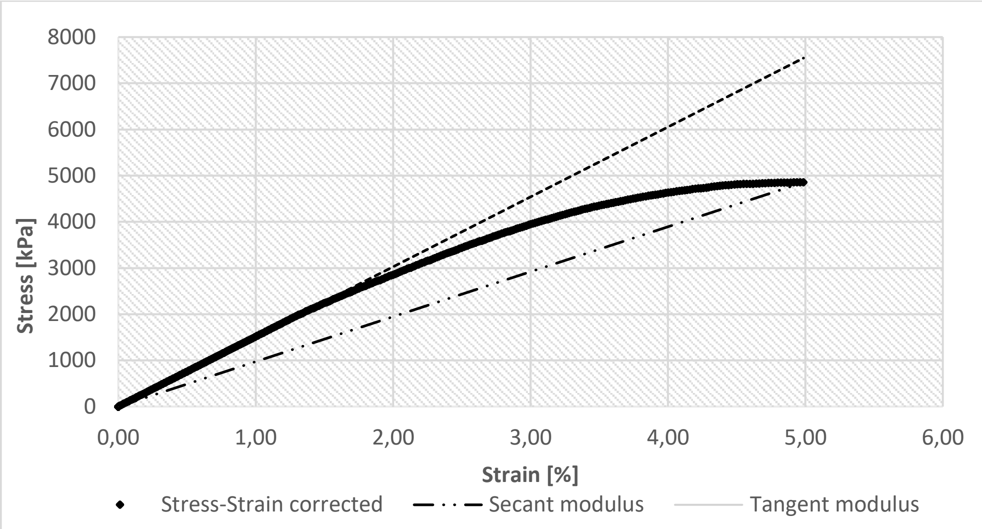

Figure 87- Elastic moduli derived from the stress-strain relationship ,CBM1.3,0 S1

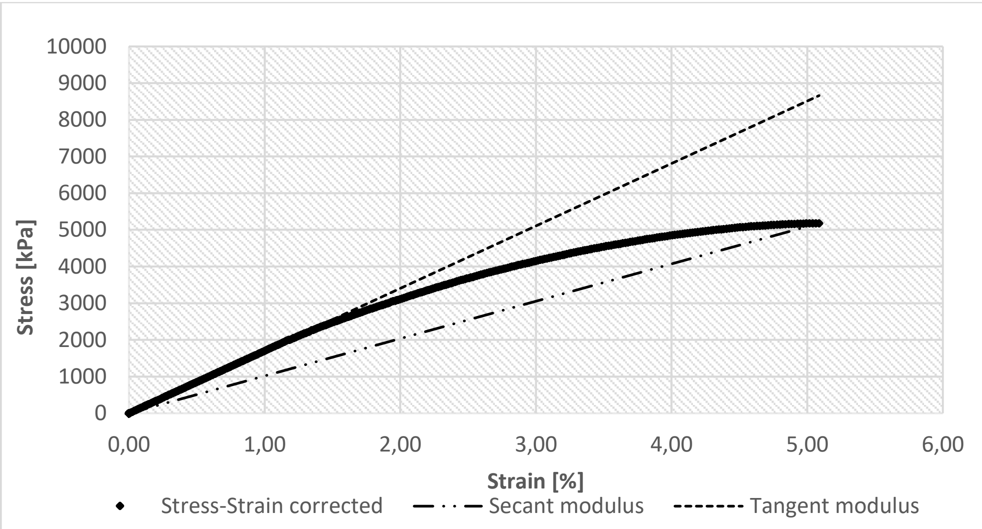

Figure 88- Elastic moduli derived from the stress-strain relationship ,CBM1.3,0 S2

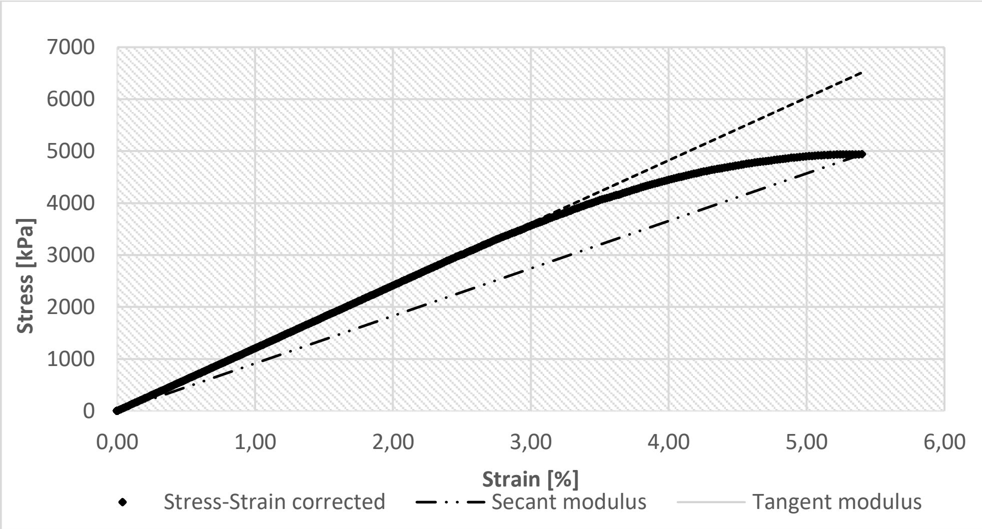

Figure 89- Elastic moduli derived from the stress-strain relationship ,CBM1.3,0 S3

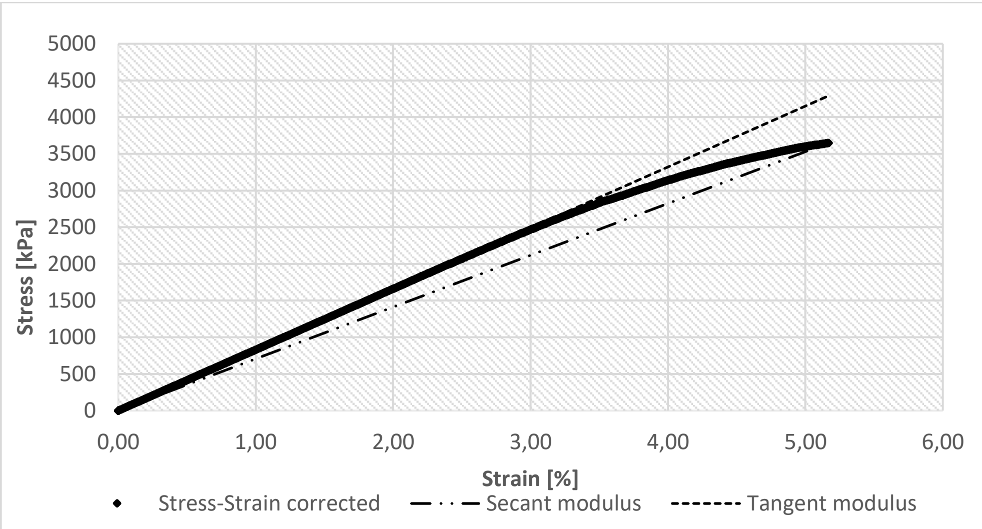

Figure 90- Elastic moduli derived from the stress-strain relationship ,CBM4.1,5 S1

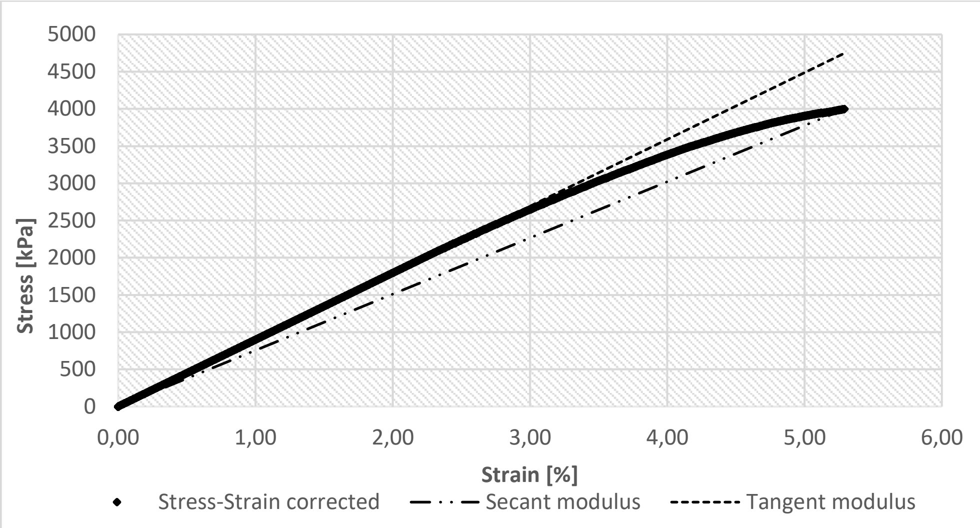

Figure 91- Elastic moduli derived from the stress-strain relationship ,CBM4.1,5 S2

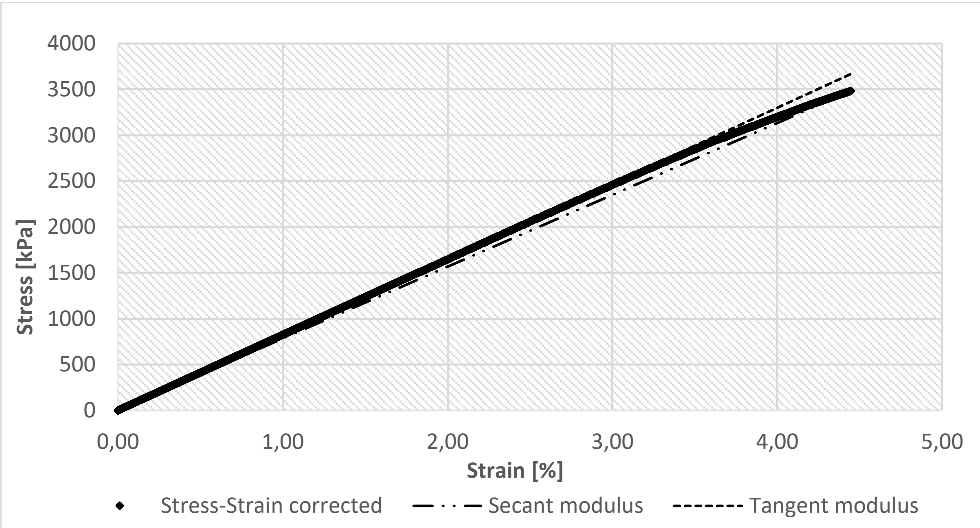

Figure 92- Elastic moduli derived from the stress-strain relationship ,CBM4.1,5 S3

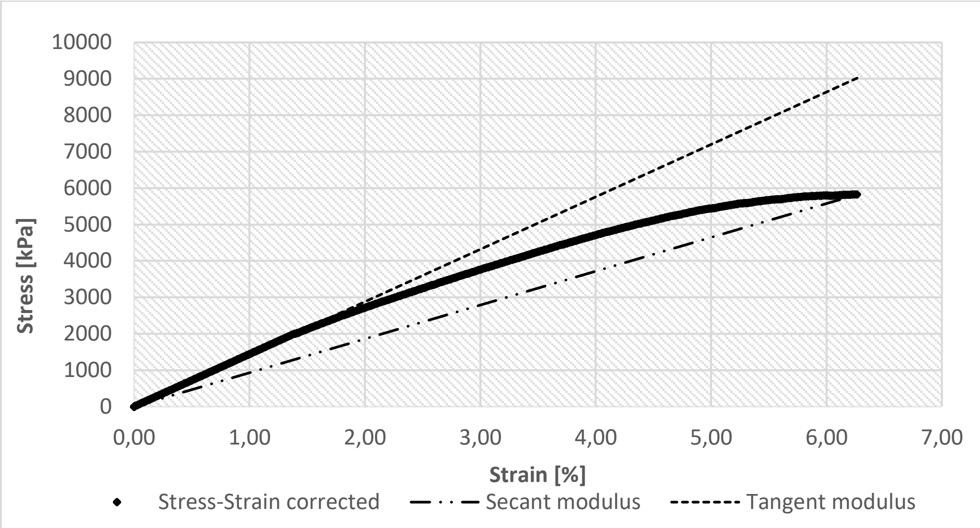

Figure 93- Elastic moduli derived from the stress-strain relationship ,CBM4.2,0 S1

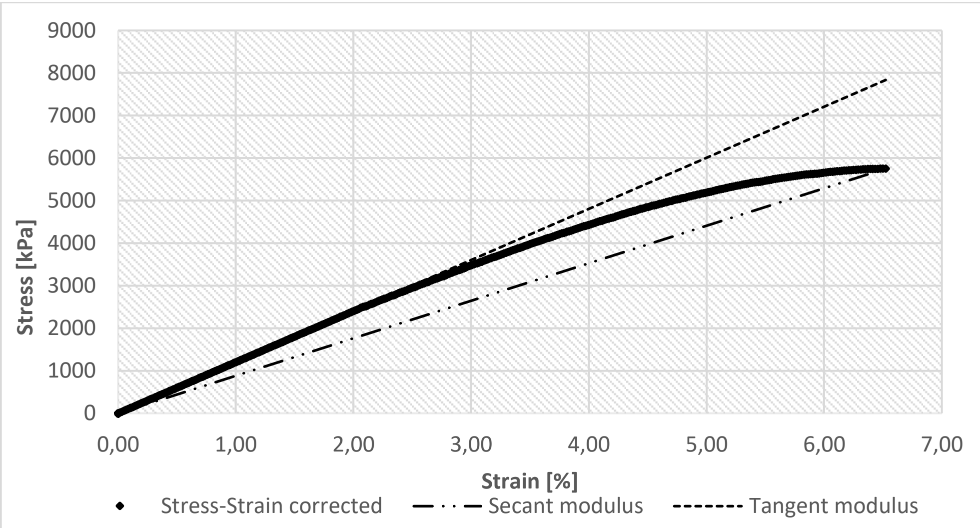

Figure 94- Elastic moduli derived from the stress-strain relationship ,CBM4.2,0 S2

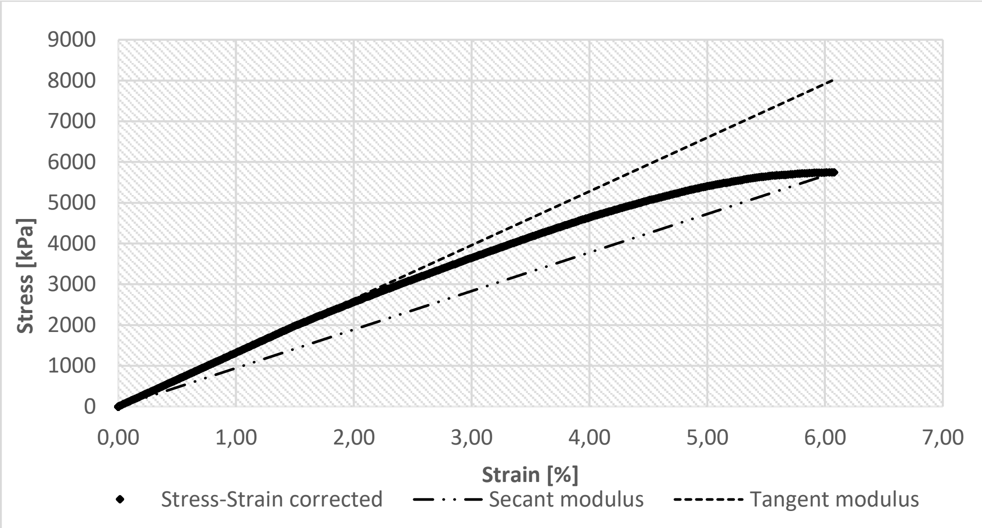

Figure 95- Elastic moduli derived from the stress-strain relationship ,CBM4.2,0 S3